quantum reports

MDPI

Review

Evidence of Predictive Power and Experimental Relevance of Weak-Values Theory

C. Aris Chatzidimitriou-Dreismann

Institute of Chemistry, Sekr. C2, Faculty II, Technical University of Berlin, D-10623 Berlin, Germany; chariton.dreismann@tu-berlin.de; Tel.: +49-30-314-22692

Abstract: The concepts of Weak Values (WV) and Two-State Vector Formalism (TSVF) appear to motivate new experiments and to offer novel insights into dynamical processes in various materials of several scientific and technological fields. To support this view, here we consider the dynamics of hydrogen atoms and/or molecules in nanostructured materials like e.g., carbon nanotubes. The experimental method applied is incoherent scattering of thermal (i.e., non-relativistic) neutrons (INS). In short, the main finding consists in the following effect: the measured energy and momentum transfers are shown to contradict even qualitatively the associated expectations of conventional scattering theory. This effect was recently observed in INS experiments, e.g., in H_2 adsorbed in carbon nanotubes, where a large momentum transfer deficit was found. Due to the broad abundance of hydrogen, these findings may be also of technological importance, since they indicate a considerably enhanced H mobility in specific structured material environments. A new INS experiment is proposed concerning the H mobility of an ultra-fast proton conductor ($H_3OSbTeO_6$) being of technological relevance. Further neutron scattering investigations on other systems (metallic hydrides and H_2 encapsulated inside C_{60}) are proposed. As concerns theoretical implications, the analysis of the experimental results strongly supports the view that the wavefunction (or state vector) represents an ontological physical entity of a single quantum system.

Keywords: weak values; Two-State Vector Formalism; incoherent inelastic neutron scattering; quantum correlations in matter; conservation laws; quantum confinement; quantum materials; proton conductors; H quantum mobility; H-surface interactions

Citation: Chatzidimitriou-Dreismann, C.A. Evidence of Predictive Power and Experimental Relevance of Weak-Values Theory. *Quantum Rep.* **2021**, *3*, 286–315. https://doi.org/10.3390/quantum3020018

Academic Editors: Manijeh Razeghi, Lajos Diósi, Lucas Lamata, Stefan Weigert, Lev Vaidman, Henry Chermette, Piero Chiarelli and Hong-Fu Wang

Received: 28 February 2021
Accepted: 30 April 2021
Published: 4 May 2021

1. Introduction

The theoretical frame of Weak Values (WV) and Two-State-Vector Formalism (TSVF) sheds more light into quantum mechanics, and provides novel insights in various physical and technological fields. Moreover, based on this theory, new experiments were suggested and various novel quantum effects were discovered; see Refs. [1–7] and references cited therein.

In this paper, the focus is not on interpretational discussions and/or new theoretical derivations; rather, we try to concentrate our attention on the question of whether the WV-TSVF theory has predictive power beyond that of the well-established and widely used standard quantum mechanics.

Moreover, an associated question is whether this theory provides any "useful" and powerful new theoretical tools that enable us to make (or create new) direct applications in already existing broad experimental fields of physical sciences. For example: Does WV-TSVF provide not only some small quantitative improvements of measurement accuracy, but a qualitatively new insight into the research (and technologically important) field of neutron scattering?

Additionally, does this new theoretical frame help our intuition and creativity in predicting new quantum effects? This point is also addressed in Ref. [8] dealing with the classical limit of quantum optics—which also stimulated our own neutron scattering

investigations reported in the present paper. e.g., as Aharonov et al. put it: "An essential point to emphasize is that this whole discussion is not just restricted to interpretations. Quite the opposite. Allowing us to have a better intuition is essential for finding new and interesting quantum effects and may lead to new experiments and potential practical applications." [8], p. 2.

In the following sections, as we believe, these (and similar) questions will be answered in the affirmative. The new effect of "momentum transfer deficit" in neutron scattering from H-containing materials represents such a quantum effect that standard theory cannot explain, as will be discussed in certain detail. Putting it in a broader context (also for the non-specialized readers), this effect and the associated presented experimental results, seem to be also of potentially technological relevance (e.g., for the technology of hydrogen storage materials, or proton mobility enhancement in fuel cells).

In the experiments under consideration in this paper, the well-established method of incoherent inelastic neutron scattering (INS, or IINS) of thermal neutrons is used. Note that INS, which uses thermal neutrons (with velocities up to a few km/s), clearly belongs to *non-relativistic* physics. The effects considered below and their theoretical treatment, especially the *momentum transfer deficit*, belong to non-relativistic quantum mechanics—and no claim is made about their validity in the relativistic regime.

Already here it should be pointed out that only *open quantum systems* are considered and/or investigated in the present paper. This "innocent" looking remark will be shown to have certain "dramatic" consequences. For instance, INS measurements from H_2 molecules enclosed in C-nanotubes—if analyzed with standard, conventional INS theory—show that the H_2 roto-translational motion along the C-nanotube axis is extremely enhanced; more precisely, the impinging neutron apparently scatters from a fictitious "molecule" having mass $M \approx 0.64$ atomic mass units (a.m.u.)—instead of the conventionally expected 2 a.m.u. for the mass of H_2. Equivalently, the momentum conservation law seems to be strongly violated here. As we will discuss below, this effect finds a natural "from first principles" interpretation in the frame of WV-TSVF theory, combined with the fact that the neutron scatters from an open quantum system.

The following short remarks regarding some common nomenclature of INS may prevent unnecessary confusion and/or misunderstandings:

(1) "Incoherent" means that each neutron collides with, and scatters from, a *single* particle (nucleus, atom, etc.). In the case of neutron scattering from protons (conventionally often referred to as H-atoms), the scattering is incoherent in a very good approximation, due to the spin-flip mechanism accompanying the neutron-proton collision [9]. This effectuates a "which-path information", thus destroying coherence between paths of the neutron originating from scattering off different nuclei. A first-principles explanation of this spin-flip effect, and of *coherent* versus *incoherent* scattering, may be found in the *"Feynman Lectures, Vol. III"* [10], particularly in Section 3.3 therein.

(2) "Inelastic" may be rather confusing in the context of a strict neutron-proton scattering. (since here the total kinetic energy of the two-body system is conserved, i.e., the collisional process is clearly elastic). This commonly used term, however, only means that the neutron's kinetic energy—i.e., the quantity recorded by the spectrometer—has changed after the collision. The same remark applies also to the neutron-nucleus scattering at the much higher energies of so-called epithermal neutrons (say, $E_0 > 10$ eV), a process belonging to deep-inelastic neutron scattering (DINS), which is synonymous with neutron Compton scattering (NCS).

(3) The INS from H using thermal neutrons represents *s-wave* scattering [9] which is isotropic.

(4) The term *effective mass* of atom A is exclusively used in the frame of, and with respect to, a non-relativistic neutron-A collision of conventional theory [9].

The paper is structured as follows:

In Section 2 we shortly consider a remarkable theoretical result of Ref. [8]—a striking exchange of momentum between a photon and a mirror of a Mach-Zehnder interferometer

(MZI). This result motivated (at least intuitively) our INS investigations. A careful consideration of the derivation of this effect shows that both WV and TSVF are used in the derivation; thus they extend standard QM and can make qualitatively new predictions—which contradicts various beliefs and/or claims of the opposite.

Section 3 and the associated Appendix B mention a few remarkable theoretical (e.g., the well-known Elitzur-Vaidman effect) and technological (e.g., the GOOGLE quantum processor) advances that support the view that the wavefunction, or state vector, is a basic, i.e., an ontic, quantity that refers to single quantum systems, and not to ensembles of systems. This view is in line with the WV-TSVF theory, which constitutes the theoretical frame for the interpretation of the striking INS effect of "momentum transfer deficit"—equivalently, a measured strong reduction of the effective mass of H—presented in the experimental Section 5.

Section 4, together with the associated more extended Appendix A, provide a self-contained presentation of the experimental and instrumental details of a TOF spectrometer, being needed in order to understand and to assess the implications of the striking experimental INS observations. This self-contained part is and essential in order to explain in full detail why the observations are "anomalous" (i.e., they have no interpretation) in the frame of standard INS theory (and, even more generally, in non-relativistic incoherent scattering theory). Here, the quantity *effective mass* in the considered specific INS experimental context is defined, and its meaning is explained with the aid of two real INS experiments (scattering from liquid ^{4}He and from protons of ice).

The theoretical interpretation of the INS experiments, based on the WV-TSVF theory, is presented in Section 6 in a concise form only, since the full theoretical treatment was very recently published in Refs. [11–13].

Section 7 deals with some proposed new experiments in order to learn more about the physics of the "momentum transfer deficit" effect, and also its potential relevance for some technological (or industrial) fields (e.g., for fast proton conductors in fuel cells).

Finally, Section 8 provides some additional discussion of various (theoretical and experimental) issues of the paper's contents, as well as short concluding remarks supporting the new predictive power of WV-TSVF and its broader applicability in various fields.

2. Theoretical Motivation

The central issue of this paper concerns (i) results of *momentum* and *energy* transfer measurements in real incoherent neutron scattering (INS) experiments, (ii) the associated predictions of conventional (classical or quantum) theory and, in particular, (iii) the comparison of the experimental INS results with a new theoretical expectation based on, and motivated by, the theory of Weak Values (WV) and Two-State-Vector Formalism (TSVF). Point (iii) has been intuitively motivated by intriguing results presented in a recent theoretical paper entitled "The classical limit of quantum optics: Not what it seems at first sight" by Aharonov et al. [8].

A particularly motivating result of [8] concerns a striking non-conventional momentum exchange between two quantum objects—a photon impinging on a small mirror of a MZI—combined with suitable post-selection of the final neutron's state, cf. Figure 1. This bears some analogy, at least intuitively, with various neutron-proton collision (or scattering) experiments considered recently [11,12,14] and in the present paper.

What is also remarkable in the derivations of Ref. [8] is that they require absolutely no previous knowledge of WV and TSVF theory, yet they succeed to demonstrate straightforwardly how the concept of WV appears naturally in the analysis of the physical problem under consideration.

Let us outline a particularly striking theoretical result of [8], i.e., a striking momentum exchange between the photon and one of the mirrors of MZI.

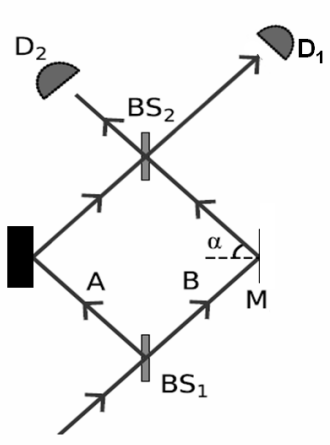

Figure 1. Mach-Zehnder interferometer and path of a photon (neutron, quantum particle). The two beam splitters are identical and have non-equal reflectivity r and transmissivity t, both being real, and subject to the condition $r > t$. The mirror M on the right is a mesoscopic *quantum* object. Of particular interest are the photons (particles) emerging toward detector D_2. (Adapted from of [8]).

Single photons (or particles) enter a device similar to a usual MZI, with the exception that one reflecting mirror is sufficiently small (say, a meso- or nanoscopic quantum object M) in order that its momentum distribution may be detectable by a suitable non-demolition measurement. With the aid of a fully self-contained and remarkably short derivation, the authors derived from first principles the following astonishing result:

Let us select those single-photon experiments, in which the outgoing photons are measured with detector D_2 and ask for the action of these photons on the (say, mesoscopic) mirror M, which should be subject to quantum mechanics. It turns out that, although the post-selected photons—as all photons do, of course—collide with the mirror M only from the *inside* of the MZI, they do not push M outwards, but rather *pull it in*! Undoubtedly, this theoretical result does not have any classical interpretation. As Aharonov et al. put it: "This is realized by a superposition of giving the mirror zero momentum and positive momentum—the superposition results in the mirror gaining negative momentum." (A concise derivation is given in [12]).

It is instructive to realize how the theory of WV (and TSVF, as we will see below,) appears naturally in this derivation, and therefore, it is necessary to point out a few formal details and/or analytic steps:

When a photon impinges from the left on the beam splitter BS_1, see Figure 1, the effect of the beam splitter is to produce inside the interferometer the state $|\Psi\rangle = ir|A\rangle + t|B\rangle$ where $|A\rangle$ and $|B\rangle$ denote the photon propagating along the A and B arms of the interferometer, respectively. See caption of Figure 1 for further notations.

The second beam splitter, BS_2, is identical to the first, *and so one can readily check that a photon in the state*

$$|\Phi_2\rangle = -ir|A\rangle + t|B\rangle$$

emerges towards detector D_2 only; see [8], p. 3. The explanation in italics will be of crucial importance in the following Section 2.1.

Let $\mathbf{P}_B = |B\rangle\langle B|$ be the *projection operator* on the photon's state to follow the path B of the MZI, see Figure 1.

If $\phi(p)$ is the initial quantum state of the mirror M and $|\Psi\rangle$ is the quantum state of the photon before reaching M, the reflection on M results in the transition

$$|\Psi\rangle\phi(p) = (ir|A\rangle + t|B\rangle)\phi(p) \to ir|A\rangle\phi(p) + t|B\rangle\phi(p-\delta) \quad (1)$$

Given $\delta > 0$ to be sufficiently small, one may make a perturbative approximation of the total state of the photon and M mirror just before the photon reaches the output beam splitter BS_2:

$$|\Psi\rangle\phi(p) \approx ir|A\rangle\phi(p) + t|B\rangle\Big(\phi(p) - \frac{d\phi(p)}{dp}\delta\Big) = |\Psi\rangle\phi(p) - t|B\rangle\frac{d\phi(p)}{dp}\delta \tag{2}$$

Now one considers a photon emerging towards D_2, after passing BS_2. The state of the mirror M is then obtained (up to normalization) by projecting the joint state onto the state of the photon corresponding to the aforementioned selected final state Φ_2, i.e.,

$$\langle\Phi_2|\Big(|\Psi\rangle\phi(p) - t|B\rangle\frac{d\phi(p)}{dp}\delta\Big) \tag{3}$$

A short derivation(see [8] or [12]) yields the result

$$\langle\Phi_2|\Big(|\Psi\rangle\phi(p) - t|B\rangle\frac{d\phi(p)}{dp}\delta\Big) = \langle\Phi_2|\Psi\rangle\phi(p - P_B^w\delta) \tag{4}$$

Here appears the term

$$P_B^w = \frac{\langle\Phi_2|\mathbf{P}_B|\Psi\rangle}{\langle\Phi_2|\Psi\rangle} \tag{5}$$

which represents the WV of $\mathbf{P}_B$ taken between the initial state $|\Psi\rangle$ and the selected final state $|\Phi_2\rangle$.

The numerical value of P_B^w is straightforwardly calculated to be

$$P_B^w = \frac{\langle\Phi_2|\mathbf{P}_B|\Psi\rangle}{\langle\Phi_2|\Psi\rangle} = -\frac{t^2}{r^2 - t^2} \tag{6}$$

Furthermore, the momentum kick (δp_M) received by the mirror due to a photon emerging towards D_2 is calculated to be

$$\delta p_M = P_B^w\,\delta = -\frac{t^2}{r^2 - t^2}\,\delta < 0 \tag{7}$$

The last inequality represents the novel result under consideration, and it holds due to $r > t$.

The appearance of the WV of the projector $\mathbf{P}_B$ in the expressions of the derivation is a characteristic feature of the WV theory. Namely, the quantum mirror M is a device "measuring" whether or not the photon (here: the system) is in arm B. The momentum of the mirror acts as a so-called pointer variable (no kick: the photon is in arm A; kick: the photon is in arm B). However, since the photon can only change the momentum of the mirror (pointer) by far less than its spread, we are in the so called "weak measurement" regime.

Furthermore, M and the photon are both quantum systems, and their interaction creates quantum correlations between them which survive their spatial separation until detector D_2 makes a strong (projective) measurement and produces a classical record (i.e., a "klick").

Concluding, the quantum-theoretical insight obtained here—the "anomalous" negative momentum transfer on M—is dramatically different from the classical (or conventionally expected) one.

2.1. A Digression: Is the Result Based on WV Theory Alone, or on Both WV and TSVF?

In this paper, WV and TSVF are considered to go beyond standard QM. However, there are differing opinions too. For instance, on may argue as follows. The WM framework is entirely contained within standard QM, and so the WV is considered to be an application of standard perturbation theory of QM. On the other hand, TSVF appears to be only a specific *interpretation* of pre- and post-selected system states (which of course is different

from the standard Copenhagen interpretation of QM). Therefore, WV and TSVF should be distinguished and their possible significance separately investigated.

Therefore, it is revealing to consider here explicitly the following question: Is the derived striking effect, inequality (7), due to the quantum theory including WVs, but without making use of the concepts of TSVF?

From first sight, the derivation of the striking result (7) in the original work [8] uses only perturbation theory (here: a simple Taylor expansion and keeping the linear term only) and concepts of standard QM.

However one should observe the following: A photon starting at D_2, after entering the MZI at BS_2 has the wavefunction $|\Psi\rangle' = +ir|A\rangle + t|B\rangle$. But this is equal to the wavefunction $|\Phi_2\rangle$ running backward in time, (the time is not explicitly shown and thus only i is replaced with $-i$). Thus the WV, Equation (1), uses the backward-in-time evolving final-state wavefunction starting at D_2. In other words, we realize that the TSVF has been used here.

Going a little further, one may observe that, according to the orthodox (or standard) interpretation of QM, the state Φ_2 does not exist—despite the innocent looking justification that it describes a photon emerging towards detector D_2. In other words, according to standard view of QM, the photon's state within the MZI (i.e, after BS_1 and before reaching BS_2) is only $|\Psi\rangle = ir|A\rangle + t|B\rangle$.

To our opinion, these considerations support once more the novel character and predictive power of WV-TSVF.

3. Short Remarks on the Logical-Axiomatic Status of "Wavefunction"

As already mentioned above, "interpretational issues" of quantum mechanics, WV and TSVF, and especially of the term "wavefunction" (or state vector; we do not differentiate between the two here) are outside the scope of this paper. Nevertheless, the experimental findings and their theoretical interpretation presented below, appear to shed some more light on such issues. Especially, the discussions of the experimental INS results seem to provide further evidence that the concept of wavefunction represents a fundamental property of single quantum systems.

The interested reader may find in Appendix B a few examples of selected additional theoretical and also technological advances, which, in our view, do support this interpretational view. For instance, it will be argued that the wavefunction represents a physical entity of a *single* system, being as real as its energy or momentum—and not of an ensemble of systems.

4. Experimental Context and Conventional Theory

This section and the associated Appendix A are essential in order to demonstrate in full detail why the INS observations considered below are "anomalous" in view of, i.e., they have no interpretation within, standard INS theory.

Moreover, here is also explained in full detail what exactly means the term *effective mass* (M_{eff}) in the here considered *specific INS experimental context*, i.e., neutron-proton scattering. This detail seems necessary, in order to prevent possible confusion with the many different definitions of "effective mass" appearing in the frames of other physical fields and/or contexts, (e.g., theory of electrons and holes in band structures), and where a small, or even a negative, value of it represents no anomaly at all. Such well known effects can be found in textbooks of solid state physics, see e.g., [15].

4.1. INS Measurement—Outline of Some Concepts

The method applied in most of the following experiments is INS, and the associated spectrometers are time-of-flight (TOF) instruments. In Appendix A are presented all essential technical details of an INS TOF-spectrometer, and a concise description of "what is directly measured" in a real INS TOF-experiment—a key point for the understanding of the experimental observations.

In this section we present some theoretical results of conventional neutron scattering theory [9,16,17], which are needed for the interpretation of the INS experiments under consideration.

4.2. Momentum and Energy Conservation in Non-Relativistic Two-Body Collisions—Conventional Theory

Let us consider a neutron colliding with an atom (better: nucleus) of mass M, using the notations defined in Appendix A. The collision is impulsive, governed by the ultashort-range (ca. femto-meter) strong force as captured by the Fermi pseudo-potential [9].

The atomic initial momentum $\mathbf{P}$ causes the energy transfer $E = E_0 - E_1 \equiv \hbar\omega$ being transferred from the neutron to the atom (E_0: neutron's initial energy; E_1: neutron's final energy; see Figure A1 of Appendix A):

$$E = E_0 - E_1 \equiv \hbar\omega = \frac{(\hbar\mathbf{K} + \mathbf{P})^2}{2M} - \frac{\mathbf{P}^2}{2M} = \frac{(\hbar\mathbf{K})^2}{2M} + \frac{\hbar\mathbf{K}\cdot\mathbf{P}}{M} \tag{8}$$

which represents the conventional energy conservation in a collision of two mass points. $\hbar\mathbf{K}$ is the momentum transfer from the neutron to the atom. In the following we use the common notation $|\mathbf{X}| = X$, for any vector $\mathbf{X}$.

The first term in the right-hand side (rhs) of the last equation is called recoil energy,

$$E_{rec} = \hbar\omega_{rec} = \frac{(\hbar K)^2}{2M} \tag{9}$$

which is the gained kinetic energy of a struck atom being initially at rest. Since $\langle P\rangle = 0$ before collision (i.e the atom is initially at rest), one obtains for the involved mean values:

$$\langle E\rangle = \frac{\hbar^2\langle K\rangle^2}{2M} \equiv E_{rec} \tag{10}$$

(Note that, for simplicity, both last equations are often used to define the same quantity "recoil energy".) This equation refers to the center of a measured peak, which usually has a finite width. Thus, INS from a gaseous sample of atoms leads to an intensity peak centered at energy transfer E_{rec}, and having a finite width caused by the additional term $\hbar\mathbf{K}\cdot\mathbf{P}/M$, which represents the well known *Doppler* broadening (see details in the Appendix A).

For illustration of the above equations, Figure 2 shows experimental data of incoherent neutron scattering from liquid helium, ^{4}He; for details see [18].

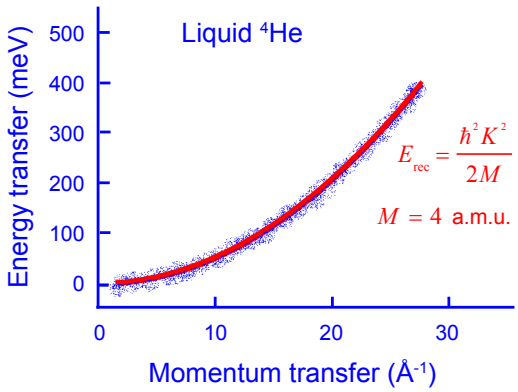

Figure 2. Schematic representation (blue points) of the dynamic structure factor $S(K, E)$ of liquid helium, adapted from Ref. [18]. The experiment was performed with the 2-dimensional TOF-spectrometer ARCS [19]. Red line: The calculated recoil parabola, Equation (10), for the mass of ^{4}He. The data are fitted with the recoil parabola with $M = 4$ a.m.u. excellently. (Figure taken from Ref. [11] with permission of Quanta).

A theoretical result illustrating the same effect is given by the calculation of $S(K, E)$ of a quantum harmonic oscillator (modeling INS from H of the palladium-hydrogen system) by Kofu and Yamamuro [20]; see Figure 6 therein.

The above simple formulas capture the main features of the so-called *Impulse Approximation* (IA) [11,16]. The IA describes ultrafast two-body collisions, since the Fermi pseudo-potential of the neutron-nucleus collision is very short (in the 10^{-15} m range) [9,16].

4.3. Experimental Determination of the Mass of the Scattering Nucleus

Small deviations from the IA, often called *final-state effects* (FSE), may be observed in experiments, which however are well understood (see, e.g., [11,16]) as follows.

When a particle with mass M is interacting with its environment, the impinging neutron effectively scatters from a particle having effectively a *higher* mass than M. This is because the adjacent particles are exerting attractive forces on the scattering particle, the free motion of the latter can only be hindered by these forces. (Repulsive forces would spontaneously separate the considered atom from its environment.) Obviously, within conventional theory, this can only lead to and increase—and never a decrease—of its *effective* mass M_{eff}

$$M_{eff} \geq M \equiv M_{free}. \tag{11}$$

cf. [11,12,16] for more details.

This inequality also follows more formally from the aforementioned energy conservation relation, if one includes an additional term $E_{int} > 0$ caused by the atom-environment interactions:

$$\bar{E} = \frac{\hbar^2 \bar{K}^2}{2M} + E_{int}, \tag{12}$$

$\bar{E}$ and $\bar{K}$ refer to the center of a measured recoil peak. Thus there is a reduced amount of energy, $\bar{E} - E_{int}$, available to the atom as its kinetic energy after the collision. $\bar{E}$ and $\bar{K}$ are determined from the neutron-atom collisional kinematics, in contrast to E_{int}, which is a quantity of the sample (i.e., of the scatterer).

Moreover, having in mind the impulsive character of the neutron-proton and the small range (about 10^{-15} m) of the strong nuclear force, one can try to fulfill this equation by using the H-mass as a fitting parameter (M_{eff}), as follows:

$$\bar{E} = \frac{\hbar^2 \bar{K}^2}{2M_{eff}}. \tag{13}$$

Here, energy and momentum transfers are assumed to be equal to the corresponding measured quantities; see also Appendix A. Obviously, the last two equations imply necessarily

$$M_{eff} > M \tag{14}$$

Again, these considerations are fully in line with conventional theory of INS. It should be emphasized that the quantity M_{eff} introduced here, which refers to the non-relativistic impulsive collision of two mass points (here; neutron and proton), is fully unrelated with other definitions of the term "effective mass" used in other fields, e.g., in traditional solid state physics [15].

The above conclusion can be reformulated to be applicable to a visual inspection of a given experimental intensity map $S(K, E)$ of an *incoherent* scattering experiment. Namely, the recoil parabola of a free atom with mass M divides the momentum-energy transfer plane $K - E$ into two parts:

- *Normal Part*. The part to the right (and thus also below) of the recoil parabola, is the conventional scattering regime, which corresponds to the discussed case $M_{eff} > M$ and thus has a conventional interpretation. Of course, the recoil parabola itself belongs to this part, too.

- *Anomalous Part*. The part to the left (and thus also above) of the recoil parabola is the non-conventional, or "anomalous", scattering regime, since it corresponds to the case of $M_{eff} < M$ which has no interpretation within standard (or conventional) INS theory.

For convenience, let us summarize here the indispensable assumptions of *conventional* INS theory, which conventional expectations are based on:

($A1$) The neutron-nucleus collision is impulsive, due to short Fermi pseudo-potential describing the strong nuclear a force.
($A2$) The collision is a non-relativistic two-body process between two mass points (i.e., neutron and the H-nucleus).
($A3$) Energy and momentum transfers hold for this two-body process.
($A4$) Prior to collision the scatterer is in thermal equilibrium (and consequently, E_{int} cannot be negative).
($A5$) The first-order quantum perturbation theory, and specifically *Fermi's Golden Rule*, which the standard INS theory is based on [9], are sufficient approximations.

In other words, it holds:

- All experimental results satisfying conventional theory must lie in the normal part of the $K-E$ plane, in which holds $M_{eff} \geq M$. Violation of relation 11, i.e., $M_{eff} < M$, is tantamount to violation of at least one of conditions $A1$–$A5$.

For further experimental results and associated details of FSE and effective mass, the interested reader may consult Refs. [11,13,16] and references therein.

4.4. INS from Bulk Ice—Validity of Conventional Theory

For further illustration of the concepts and relations of the preceding subsection, let us consider here one more experimental result: INS from H of H_2O molecules of ice. INS from H-containing samples is usually done at very low temperatures, because this reduces the "background" (due to phonons, librations etc..) and Debye-Waller-factor effects [9] on the measured $S(K,E)$. The latter is the quantity of primary interest for quantifying material properties and testing theoretical predictions [9].

Figure 3 shows the experimentally observed $S(K,E)$ of micro-crystalline ice Ih at $T = 20$ Kelvin and 1 bar pressure [21], using the TOF spectrometer MARI [22] of ISIS neutron spallation source, UK. Neutron's initial energy was $E_0 = 750$ meV. The most significant scattering contributions are caused by H, which has a much larger incoherent scattering cross-section than other atoms [9]. The black parabola line represents the conventional recoil line of a free H, i.e., with effective mass ≈ 1 a.m.u., being initially at rest

$$E_{rec}^{free} = \frac{\hbar^2 K^2}{2M_H} \tag{15}$$

(M_H: atomic mass of H.) Recall that H and neutron (n) have almost equal masses, $m_n \approx M_H$. Clearly, this is equivalent to the preceding Equation (10).

The intensity peak around $E = 420$ meV and $K = 14$ Å^{-1} is due to the molecular *stretching OH-vibrational* modes of H_2O. Note that the center of intensity peak lies on the free H-atom recoil line, as conventionally expected. In view of Equation (15), this experimental result shows that the observed intensity peak is well described with the common theoretical assumption that the collision is impulsive and essentially a two-body process. I.e., a "dressing" of the vibrationg H with environmental and/or intramolecular degrees of freedom is not relevant, and we have $M_H^{eff} = M_H^{free} \approx 1.0$ a.m.u.—as conventionally expected. Thus, as stated in the preceding subsection, the stretching vibrational peak lies in the "normal part" of the $K-E$ plane.

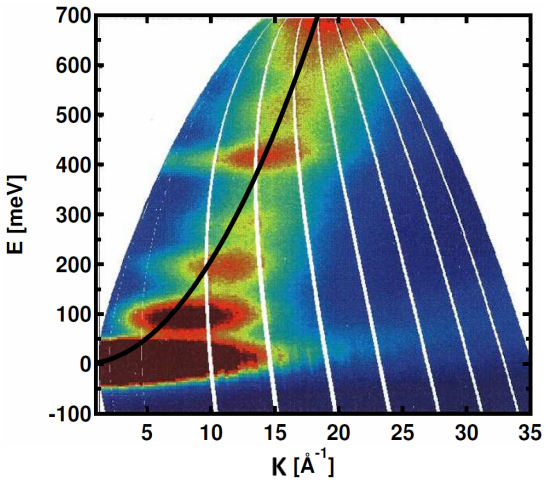

Figure 3. Measured $S(K, E)$ intensity map of ice Ih at 20 K and 1 bar, recorded on MARI [22]. $E_0 = 750$ meV. The shown black line (parabola) is the conventional recoil trajectory of a free H. The strong intensity ribbon at $E \approx 0$ is mainly due to the aluminum cell containing the water (ice). The intensity peak maximum at $E \approx 420$ meV and $K \approx 14$ Å^{-1} represents the vibrational stretching OH-vibrations. (Reproduced from Ref. [21] with permission).

In this context, Kearley et al. [23] gave the following additional justification to the above physical picture: The very short (roughly in the pico- to femto-second) neutron-H scattering time, taken together with the significant spectral separation of the stretching modes from the other modes, effectuate a decoupling of the "fast" H-stretching motion from the other (slower) ones.

We observe a slightly different behavior of the *bending* vibrational mode, which gives the peak at energy transfer $E \approx 200$ meV. Obviously, this peak is centered to the "right" of the H-recoil parabola, i.e., it is still in the "normal part" of the $K - E$ plane.

Applying the aforementioned argument by Kearley et al. [23] we can also provide the following conventional explanation: The bending motion is hindered by adjacent H-bonded molecules, and thus the scattering atom is "dressed" by environmental degrees of freedom, which causes an increased effective H-mass. Indeed, a rough estimate derived from the peak-center position of the $S(K, E)$ graph, Figure 3, yields for the effective mass of the struck H in the bending mode: $M_H^{eff} \approx 1.3$ a.m.u.

Summarizing, the above INS observations about the HO-vibrations of ice have a straightforward conventional-theoretical interpretation. Surprisingly, in the next section we will see that this is in blatant contrast to the case of H_2O molecules being in certain nano-scale confinements, where the stretching vibrational mode of H_2O exhibits a significantly large anomaly, as originally noticed in [21].

5. The New Scattering Effect—Momentum Transfer Deficit on H

5.1. First Example: INS from Single H_2 Molecules in C-Nanotubes

In some experimental explorations in the field of material sciences, a surprising INS result was recently discovered [24]. This concerns the quantum excitation spectrum of H_2 adsorbed in multi-walled nanoporous carbon. The C-nanotubes had pore diameters about 8–20 Å.

These experiments were carried out at $T = 23$ Kelvin with the TOF-spectrometer ARCS of SNS [19]. Note that the energy transfers in this experiment cannot excite H_2-vibrations (which lie much higher), but only rotations and translations only. Thus it holds

$$E = E_{rot} + E_{trans}. \tag{16}$$

The experimental two-dimensional INS intensity map $S(K, E)$ of H is shown in Figure 4b [24]. The following features should be noted. The intensive peak at $E_{rot} \approx 14.7$ meV

is due to the first rotational excitation $J = 0 \rightarrow 1$ of H_2 [17]. The observed momentum transfer of this peak is $K_{rot} \approx 2.7$ Å^{-1}. Thus the peak position in the $K - E$ plane satisfies the relation $E_{rot} = (\hbar K_{rot})^2/2M_H$ with the mass M_H of the free H atom,

$$H_2 \text{ rotation } (J = 0 \rightarrow 1): \quad M_{eff} = M_H = 1.0079 \text{ a.m.u.} \tag{17}$$

In other words, the spectral position of this rotational excitation is fully in line with conventional theoretical expectations. And since the scattering is incoherent, one may say that each neutron scatters from a single H atom.

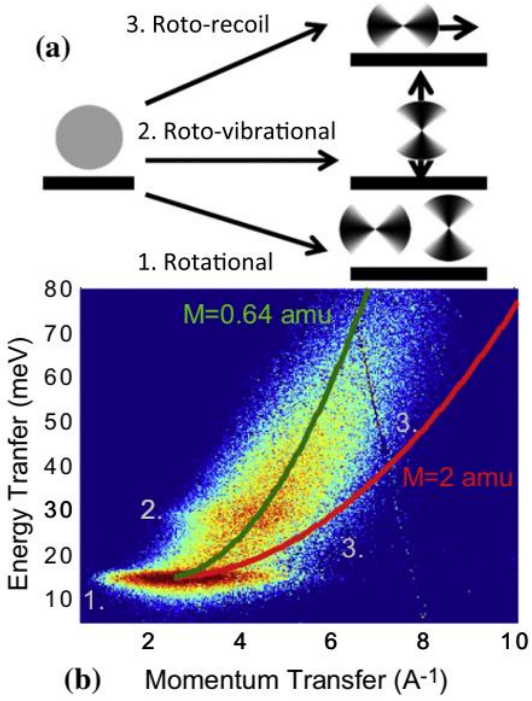

Figure 4. (**a**) Schematic representation of various molecular motions of H_2 in a nanotube, as conventionally expected. (**b**) Experimental INS results from H_2 in C-nanotubes. Incident neutron energy: $E_0 = 90$ meV; [24]. The translation motion of H_2 molecules is attributed to the observed continuum of intensity, also termed "roto-recoil" (yellow-orange ribbon). The $K - E$ position of the first rotational excitation of H_2 (dark red-brown ellipsoid) is in accord with conventional theory. In contrast, a blatant disagreement with conventional theory holds for the roto-recoil data: A fit (green parabola) to this yields the effective mass $M_{eff} \approx 0.64$ a.m.u. for the translating H_2 molecule. The red parabola on the right shows the conventionally expected recoil parabola for the H_2-mass which is $M = 2$ a.m.u. (Reproduced from [24], with permission of Elsevier Ltd.).

Moreover, the novel finding of [24] is as follows. A detailed numerical treatment of the roto-recoil data (cf. Figure 4) was presented, which derived a significantly reduced effective mass of the recoiling H_2 molecule (left parabola, green):

$$H_2 \text{ translation (recoil):} \quad M_{eff}(H_2) \approx 0.64 \pm 0.07 \text{ a.m.u.} \tag{18}$$

Additional INS experiments with differing C-nanotube samples showed no significant variation of this astonishing numerical value. Obviously, this experimental result is in blatant contradiction to the value $M(H_2) = 2.01$ a.m.u. for a freely translating H_2 molecule (right parabola), as conventional theory predicts.

This observation provides direct evidence for the new "anomalous" effect of $\hbar K$-transfer deficit [11,21].

According to the associated discussions above (see Section 4.3), every conventional H_2/substrate binding (or interaction) can never decrease the effective mass of the molecule. Thus these INS results contradict conventional theoretical expectations. However, we will see below that they find a natural interpretation in the WV-TSVF theoretical frame.

5.2. Second Example—INS from Single H_2 Molecules in the Metal-Organic Framework Material "HKUST-1"

Due to its considerable magnitude and its surprising character, it is important to have another, fully independent, confirmation of this effect.

Other INS experiments, with the goal to discover novel materials for potential use in the technology of storage and transport of hydrogen, investigated the adsorption of H_2 on various porous metal–organic framework materials over the past few years. The material known as HKUST-1 (see [25] for its chemical stochiometry and crystalline structure) has emerged as a characteristic model system for related studies. Here it suffices to note that HKUST-1 constitutes a three-dimensionally connected network, with a trimodal pore structure, having pores with diameters in the range 5–12 Å.

Also in his material, the experimental intensity map $S(K, E)$ shows again a broad band attributed to the translational H_2-motion in the pores, which is very similarly to the experiment presented in the preceding subsection. Again, the measurements were done at low temperatures, $T < 30$ Kelvin [25].

5.3. Comparison of the Two Experiments

Most importantly, the experiment [25] provides an independent confirmation of the striking result of Ref. [24] obtained at SNS, USA. The INS measurements of Ref. [25] were done with the 2-dimensional spectrometer MARI (ISIS facility, UK)—that is, by an independent European group of scientists, and in a different laboratory.

Figure 5 permits a direct visual comparison of the data of the two experiments, which reveals a reassuring result. Namely, The two broad continuous bands due to the translational mode are virtually identically positioned in the $K - E$ plane. This is quite astonishing given the fact that the two experiments were done with two different nano-structured materials.

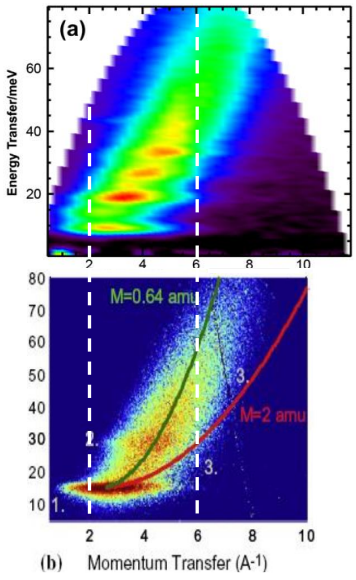

Figure 5. Experimental intensity maps $S(K, E)$ of the two original results of [25] (**a**) and [24] (**b**), appropriately stretched/scaled to facilitate visual comparison. The two vertical dashed lines (white) are guides to the eye. The two broad continuous features caused by the roto-translational modes are virtually identically distributed in the $K - E$ plane, and they clearly lie in the quantum regime, i.e., on the "left" of the H-recoil parabola of H. (Figure taken from Ref. [14]).

Therefore, we may expect that the observed effect should be present in far more materials than known until now.

6. Theoretical Interpretation within WV and TSVF Theory

In this section, we present an outline of our recently published [11,12] theoretical model in the frame of WV-TSVF theory, which explains from first principles the anomalous momentum-transfer deficit observed in the preeceeding experiments. For full details of derivations, see [11,12].

We re-consider Equation (8) capturing E-conservation in a strict two-body collision. Due to momentum conservation, one expects (n: neutron; A: atom)

$$-\hbar K_n = +\hbar K_A \equiv \hbar K > 0, \tag{19}$$

where $+\hbar K_A$ is the momentum transfer *on the atom*. Following standard notation (e.g., as in [9]) we choose K_A to be positive.

Having the theory of WV and TSVF in mind, one sees that the "larger" recoil term $(\hbar K)^2/(2M)$ may be viewed to result from a *strong* impulsive interaction (associated with momentum transfer $+\hbar K$ on the atom). In the IA holds $|K| \gg |P|$, and thus the "smaller" *Doppler* term $\hbar\mathbf{K}\cdot\mathbf{P}/M$ corresponds to a *weaker* interaction, in which the atomic momentum $\hat{P}$ couples with an appropriate dynamical variable of the neutron; the latter turns out to be $\hat{q}$ [11].

In view of the theory of WV and TSVF, the mentioned smaller Doppler term is expected to cause weak *deviations* from the conventionally expected momentum transfer $+\hbar K$. This can be formally captured by replacing $\hat{P}$ with a *small* momentum difference $\hat{P} - \hbar K\hat{I}_A$ ($\hat{I}_A$: identity operator in the atomic sub-space). For formal reasons, here is temporarily included a positive *smallness* factor, $0 < \lambda \ll 1$; see Discussion below. Summarizing, the proposed von Neumann-type model interaction Hamiltonian (describing the deviation from conventional theory) is [11]

$$\Delta\hat{H}_{int}(t) = +\lambda\,\delta(t)\,\hat{q}\otimes(\hat{P} - \hbar K\,\hat{I}_A) \tag{20}$$

($\delta(t)$: delta function; λ: small real constant). It should be emphasized that the *plus sign* in front of this expression is not arbitrary, since it is consistent with the aforementioned definitions (19) of momentum transfer; cf. [11].

The physical motivation of the two parts of the model Hamiltonian of Equation (20) is in conceptual agreement with the following associated remark by Aharonov et al.: "Consider, for example, an ensemble of electrons hitting a nucleus in a particle collider. [...] The main interaction is purely electromagnetic, but there is also a relativistic and spin-orbit correction in higher orders which can be manifested now in the form of a weak interaction." ([26], p. 3).

6.1. WV of Atomic Momentum Operator $\hat{P}$ and the Effect of "Anomalous" Momentum-Transfer Deficit

In the following, the scattering atom represents the "system" of the general formalism, and the subscript w in X_w indicates that this is a WV of the observable $\hat{X}$. The WV of the identity operator is $(\hat{I}_A)_w = 1$, and thus for the WV of the atomic coupling operator $\hat{P} - \hbar K\,\hat{I}_A$ in the above interaction Hamiltonian:

$$(\hat{P} - \hbar K\,\hat{I}_A)_w = P_w - \hbar K \tag{21}$$

To proceed, we first calculate the WV P_w of $\hat{P}$ for some characteristic final state in momentum space. The derivation reveals a striking deviation—more precisely, a deficit—from the conventionally expected momentum transfer to the neutron. The latter represents the "pointer" of the general theory, and the pointer momentum variable $\hat{p}$ is conjugated to the neutron position $\hat{q}$.

In the following we use the momentum space representation, motivated by the fact that most scattering experiments measure momenta (rather than spatial positions).

Let atom A being initially in a spatially confined state and at rest. Here we may approximate the initial atomic wavefunction $\Xi(P)_i$ by a Gaussian $G_A(P)$ centered at zero momentum, $\langle P \rangle = 0$, i.e.

$$\Xi(P)_i \approx G_A(P). \tag{22}$$

The width of $\Xi(P)_i$ is determined by the quantum uncertainty. The struck atom will move in the direction of momentum transfer $\hbar K_A = \hbar K$. Therefore, in the following calculations P may represent the atomic momentum along the direction of momentum transfer.

To make the derivations and their physical meaning more intuitively transparent, let us assume:

- The final atomic state has the same *width* in momentum space as the initial state.

This assumption is very common in molecular (optical) spectroscopy and/or quantum-chemical calculations of molecules; it corresponds to the well known Franck–Condon picture. Namely, it captures the intuitive view that the impulsive transition is very fast and so the atomic environment remains unchanged during the neutron-atom collision. Thus the final atomic momentum wavefunction should have the same shape as the initial state and it is shifted from zero to the transferred momentum, i.e.,

$$\Xi(P)_f = \Xi(P - \hbar K_A)_i. \tag{23}$$

The WV of the atomic momentum operator $\hat{P}$ is then readily calculated:

$$\begin{aligned} P_w &= \frac{\langle \Xi_f | \hat{P} | \Xi_i \rangle}{\langle \Xi_f | \Xi_i \rangle} = \frac{\int dP\, \Xi(P - \hbar K_A)_i\, P \Xi(P)_i}{\int dP\, \Xi(P - \hbar K_A)_i\, \Xi(P)_i} \\ &= +\frac{\hbar K_A}{2} = +\frac{\hbar K}{2} \end{aligned} \tag{24}$$

The evaluation of the integral in the numerator follows immediately from the following simple considerations: (a) the two functions Ξ are positioned symmetrically around the middle point $\bar{P} = \hbar K_A/2$—one function is centered at 0 and the other at $\hbar K_A$; and (b) P is a linear factor. I should be noted that this result does not depend on the width of the Gaussian Ξ.

This is a quite surprising result because it is associated with a considerable K-transfer correction of 50%; i.e., the scattered neutron measures a momentum kick being only half of the conventionally expected value, if one takes $\lambda = 1$; see also Discussion. In more detail, it holds

$$(\hat{P} - \hbar K\, \hat{I}_A)_w = +\frac{\hbar K_A}{2} - \hbar K = -\frac{\hbar K}{2} \tag{25}$$

More explicitly, applying the well-known general result of WV and TSVF [1,3,5] we obtain for the *correction* to the shift of the meter's (i.e., the neutron's) pointer variable:

$$\langle \hat{p} \rangle_f - \langle \hat{p} \rangle_i = -\lambda\, (\hat{P} - \hbar K\, \hat{I}_A)_w = +\lambda\, \frac{\hbar K}{2} \tag{26}$$

(See [11] for full derivation) Moreover, for the *total* momentum transfer shown by the pointer of the measuring device (here: neutrons) we have

$$\begin{aligned} \left[\langle \hat{p} \rangle_f - \langle \hat{p} \rangle_i\right]_{\text{total}} &= \left[\langle \hat{p} \rangle_f - \langle \hat{p} \rangle_i\right]_{\text{conventional}} + \left[\langle \hat{p} \rangle_f - \langle \hat{p} \rangle_i\right]_{\text{correction}} \\ &= -\hbar K + \lambda\, \frac{\hbar K_A}{2} \end{aligned} \tag{27}$$

This result represents the effect of *momentum-transfer deficit*: the absolute value of momentum transfer on the neutron predicted by the new theory is *smaller* than conventional (or standard) theory predicts:

$$|-\hbar K + \lambda\,\hbar K_A/2| < |-\hbar K| \tag{28}$$

Here holds the aforementioned definition: $\hbar K_A = \hbar K$, Equation (19).

6.2. Plane Waves Approximation Implies Conventional Momentum Transfer

In theoretical investigations of conventional neutron scattering theory, the plane wave approximation plays a central role. Therefore, it is of paramount importance to show explicitly the consequences of using this approximation in tthe frame of the present WV-TSVF analysis.

So let us here make the assumption:

- The final state of the struck atom should be a plane wave, i.e., it has vanishing width in momentum space—as e.g., in the IA.

Interestingly, now the well known result of conventional theory (i.e., the conventional momentum transfer $\hbar K$) follows straightforwardly within our formalism—the preceding correction due to WV and TSVF just disappears. Now the atomic final-state wavefunction of A is a delta function δ_A centered at the assumed transferred momentum $\hbar K_A$,

$$\Xi(P)_f = \delta_A(P - \hbar K_A) \tag{29}$$

For the WV of $\hat{P}$ one then obtains:

$$\begin{aligned} P_w &= \frac{\langle \Xi_f|\hat{P}|\Xi_i\rangle}{\langle \Xi_f|\Xi_i\rangle} = \frac{\int dP\,\delta_A(P-\hbar K_A)\,P\,\Xi(P)_i}{\int dP\,\delta_A(P-\hbar K_A)\,\Xi(P)_i} = \frac{\hbar K_A\,\Xi(\hbar K_A)_i}{\Xi(\hbar K_A)_i} \\ &= +\hbar K_A \equiv +\hbar K \end{aligned} \tag{30}$$

Hence, the WV of the system coupling operator, $(\hat{P} - \hbar K\,\hat{I}_A)$, becomes equal to zero, that is,

$$(\hat{P} - \hbar K\,\hat{I}_A)_w = P_w - \hbar K = 0 \tag{31}$$

Parenthetically, it may be noted that, according to standard theory, the scattered wave may acquire an additional phase factor, e.g., $e^{i\chi}$. Howeever this does not affect the preceding result because this factor cancels out in the fractions of Equations (24) and (30).

This result implies that, under the usual assumption of "plane waves", the WV-TSVF theory yields *no correction* to the conventionally expected value of momentum transfer. Hence we have:

$$\Big[\langle\hat{p}\rangle_f - \langle\hat{p}\rangle_i\Big]_{\text{total}} = \Big[\langle\hat{p}\rangle_f - \langle\hat{p}\rangle_i\Big]_{\text{conventional}} = -\hbar K \tag{32}$$

In other words, the pointer of the measuring device—i.e., the experimentally determined momentum loss of a neutron—will now exhibit the conventionally expected value $-\hbar K$. Importantly, the result of Equation (31) is consistent with conventional theory of the IA, and also of general incoherent neutron scattering theory—the standard expectation of conventional theory is here reproduced. This is a very satisfactory result.

Comparison of the aforementioned two derivations shows that the magnitude of the momentum transfer deficit under consideration depends on the "deformation" of the shape of the final atomic state. e.g., if the final state is, say, "almost" a delta function (plane wave), then the anomalous momentum transfer deficit will be "very small"—and perhaps remain undetectable. Recall that the plane-wave assumption is standard in NCS and/or DINS data analysis; cf. [16].

The general case of an arbitrary shape of the final-state wavefunction was derived and discussed in Ref. [11].

6.3. On Pre- and Post-Selection of System's States

In the physical set-up of a MZI and the *gedanken* experiment of Section 2, one recognizes easily how the theoretical concepts of pre- and post-selected states of WV and TSVF theory appear. Namely, it is clear that these states are simply chosen by the experimentalist.

In contrast, this is not the case in the theoretical model presented in this section—the experimentalist has not the capability to choose the atomic (or molecular) states of H in a material probe, like those described above, at his/her will.

First, is intuitively easy to understand that the initial (before collision) H-state corresponds to the concept of a pre-selected state in the sense of WM-TSVF. But what about the post-selected states, which, as we saw in the above model calculations, can greatly affect the magnitude of the WV of the H-momentum operator?

Looking at the INS experiments on H_2 in C-nanotubes (Section 5.1), one may realize the following details.

After neutron-H collision, the H_2 molecule can translate only along the C-nanotube axis, but not perpendicular to it. (due to the nanoscale diameter of the C-nanotube). In other words,

(1) the C-nanotube's geometry, taken together with
(2) the orientation of the sample with respect to the neutron-beam, and
(3) the associated chosen direction of the momentum transfer $\hbar\mathbf{K}$,

correspond to, or effectuate, the choice of a specific post-selection of the final state of the roto-translating H_2. And, as we saw in Figure 4, this specifically selected state may led to the dramatic effect of momentum transfer deficit (and the corresponding non-conventional result $M_{eff} < M_H$).

Furthermore, the INS results from H_2 in C-nanotubes presented above might appear contradictory, because:

(i) The $J = 0 \rightarrow 1$ rotational excitation of H_2 shows a conventional $M_{eff} \approx 1$ a.m.u.
(ii) In contrast, the M_{eff} of the observed translational roto-recoil response of the whole H_2 is not 2 a.m.u. (as expected by conventional theory because the whole H_2 undergoes a translational motion), but only $M_{eff} \approx 0.64$ a.m.u., see Equation (18).

However, This "conflict" just disappears in the light of the WV-TSVF theoretical frame, because it simply implies that the quantum *environments* $\mathcal{E}$ of H in the two cases (i) and (ii) are *different*. In illustrative terms, the locally rotating H_2 is much less influenced by its environmental interactions than the translating H_2 that necessarily interacts with a greater part of the nanotube during its translational motion initiated by the collision. In short: Different environments effectuate different post-selections of the H_2 final state.

These considerations indicate a potential applicability of these ideas in the field of material sciences. Namely, the discussed post-selected H-states are effectuated by the H-environment, i.e., the nano-structure of the host material, besides its physico-chemical properties. Further studies along these lines of thought may be of technological/industrial significance, too.

7. Expectations and/or Predictions of New Effects in Various Materials

Motivated by the striking experimental results of Section 5, we propose and/or qualitatively predict further concrete experimental topics which are expected to show similar "anomalous" momentum-transfer deficit effects. Two of them, i.e., the ultra-fast proton conductor $H_3OSbTeO_6$ and the metallic hydride system PdH_x are even of technological (industrial) relevance.

7.1. INS Investigation of Momentum Transfer Deficit on H of the Fast Proton Conductor $H_3OSbTeO_6$

In this subsection, a qualitative prediction concerning a possible technological application is considered.

Solids with high proton mobility are of considerable technical (and industrial) interest as electrolyte materials in fuel cells working in the temperature range below 600 K. Nowadays, the commonly used so-called PEM cells, working below 373 K, are equipped with specific polymers, which are very sensible to various disturbances or inefficiencies, e.g., their intolerance to impurities, water and heat management, additionally to their high costs.

Therefore, the search for alternative fast proton conductors based on inorganic solids has been under intense investigation. In 1985, Turrillas et al. [27] reported an antimonic acid-based compound with an outstanding proton conductivity of $\sim 10^{-2}\Omega^{-1}\mathrm{cm}^{-1}$, which opened up a new road of materials research. The most promising composition of this class of materials is $H_3OSbTeO_6$, a potential candidate for advanced fuel cells technology [27,28].

This material consists of a three-dimensional interconnected (Sb,Te)O_6 framework, built from randomly distributed corner-shared SbO_6 and TeO_6 octahedra, forming large cages interconnected to a three-dimensional network, in which mobile H_3O^+ ions are contained; see Figure 6. The observed outstanding proton conductivity is due to the dynamics of these ions.

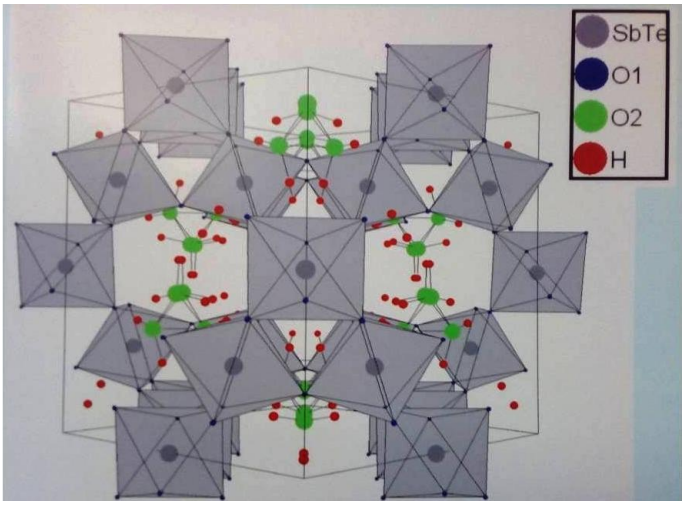

Figure 6. Crystal structure of proton conductor $H_3OSbTeO_6$.

Extensive experimental investigations with various techniques [28], accompanied by quantum chemical calculations, have identified three main types of motion of protonic species: (1) stochastic rotations of the H_3O group around its 3-fold axis, (2) jumps between four equivalent positions within the octraedral cages, and (3) long-range translational motion (diffusion) over several cages. Specific details of the complex kinetic mechanisms were given in Ref. [28]. Note that INS experiments similar to those presented in the preceding section have not been reported thus far.

Making contact with the findings of the preceding section, in the following our interest lies with the translational motion of the H_3O group (or H_3O^+-ion). Motivated by our theoretical WV-investigations on the quantum momentum transfer deficit and associated enhanced mobility of H_2, we are led to the following prediction:

- The 2-dim. $S(K,E)$ of this material should reveal an anomalous momentum-transfer deficit on H_3O^+, which may be qualitatively similar to the effect of Figure 5 shown above. The roto-translational continuum of the H_3O^+, if measurable, would be again deeply in the quantum domain of the $K-E$, i.e., it should be positioned "on the left" of the H_3O^+-recoil line. Furthermore, observation of a (howsoever weak) translational continuum of single protons (H^+) caused by neutron collisions would provide neew insights into the conductivity mechanism.

These suggested INS experiments should be carried out at incident neutron energies (1) similar to the preceding experiments, and additionally also (2) at E_0 about 1000 meV, so

that also the stretching HO-vibration can be excited and observed in a 2-dim. spectrometer (like ARCS). In the latter case,

- the stretching vibrational HO-peak is expected to lie again in the quantum regime of the $K - E$ plane similarly to the quantum effect observed on the HO-stretching vibrations of H_2O molecules in some nanoscopic channels of inorganic materials [29],

as earlier discussed and analyzed in Refs. [12–14,21]. For the convenience of the reader, here we display again the mentioned effect, as shown in Figure 7.

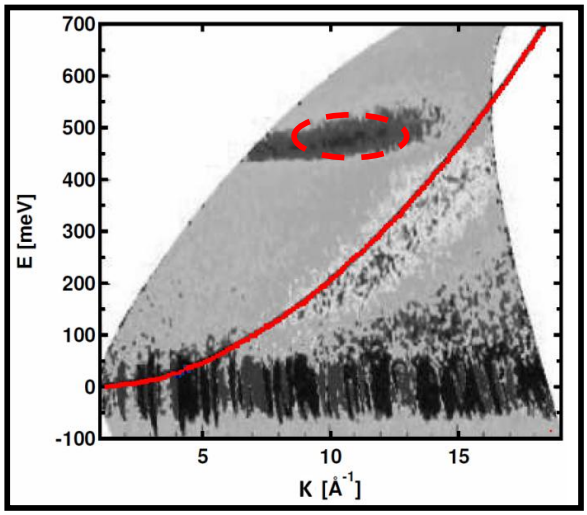

Figure 7. INS from oriented single H_2O molecules in sub-nanometer channels of beryl (chemical formula $Be_3Al_2Si_6O_{18}$) at $T = 7$ Kelvin [29], investigated with the TOF-spectrometer SEQUOIA of SNS, Oak Ridge Nat. Lab., Oak Ridge, TN, USA. Neutron incident energy was $E_0 = 800$ meV. The figure shows the difference of two measured $S(K, E)$ maps: (i) for K-perpendicular-to-c and (ii) for K-parallel-to-c orientation. Red parabola line: the calculated recoil trajectory of a free proton. The strong intensity peak at energy transfer 450–500 meV (marked with the ellipsoid, red broken line) are the well-known stretching OH vibrational modes, which exhibit a strong momentum-transfer deficit effect [21]. The molecules are oriented with their H–H direction parallel to the c-axis of the crystal's channels. (Adapted from of [29]; see also [13]).

The following specific remark may be of interest. Figure 8 shows experimentally determined widths σ_H of the momentum distributions of H in $H_3OSbTeO_6$ and of solid polyethylene at room temperature [30] recorded with the electron-Volt TOF-spectrometer eVS/Vesuvio of ISIS, Oxfordshire, UK. The scattering method is termed neutron Compton cattering (NCS), also known as deep-inelastic neutron scattering (DINS). This technique measures the momentum-peak shapes of the recoiling atoms, especially of H, and thus it determines the H-momentum distributions; see e.g., the concise review article by Watson [16].

The measured widths σ_H of the H-momentum distributions in the two materials appear to be approximately equal, which shows that the scattering H species in the two materials are covalently bonded with comparable bonding energies. Any indication of quasi-free protons (H^+) "jumping" between water molecules, and/or translating in the channels of the proton conductor $H_3OSbTeO_6$ is absent in the data. The characteristic scattering time of NCS is shorter than that of INS, due to the higher incident energies of NCS being the the range 1–100 eV. It is expected that the proposed new INS experiment on $H_3OSbTeO_6$ should show an "anomalous" vibro-translational motion of H_3O^+, in an analogous way as the INS experiments in the preceding section show the striking roto-translational motion of the H_2 molecule.

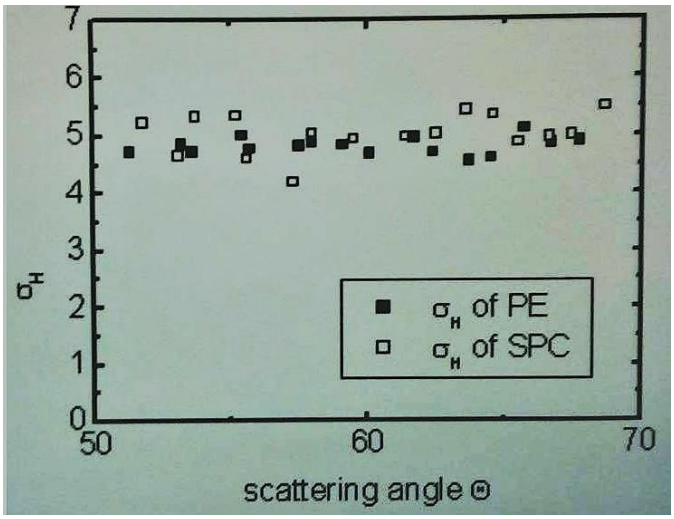

Figure 8. Measured widths σ_H (in $Å^{-1}$) of the Compton profile [16] of H in $H_3OSbTeO_6$ (SPC) and of solid polyethylene (PE) at room temperature [30]. The Compton profile is the H momentum distribution along the K-direction.

If the aforementioned prediction would be confirmed by the INS experiment, this would demonstrate that the outstanding high conductivity of $H_3OSbTeO_6$ is intrinsically connected with the quantum effect of momentum transfer deficit [11] on the H protons of H_3O^+. This knowledge would facilitate further investigations for the optimization of fast proton conductors.

7.2. INS from H of Metal-Hydrogen Systems

Structural and dynamical effects of H in various metals has attracted considerable interest in fundamental and applied research areas for many decades. For instance, Palladium (Pd) and Niobium (Nb) are interesting, because they can absorb large quantities of hydrogen, and H-atoms are highly mobile in some lattices, even at room temperature. The physical nature of this high mobility is not fully understood thus far [31]. Metallic hydrides is also of certain technological and/or industrial relevance, since they have been suggested to represent possible hydrogen storage materials at room temperature.

For example, INS has been used to study the dynamics of hydrogen in Pd (even at room temperature), and such studies provided many insights into the microscopic dynamics of H atoms in this system; see e.g., Ref. [20] and the extensive literature cited therein. Of particular interest for our purposes is the fact that, in this metallic hydride, INS takes place from *atomic* H—which extends the aforementioned class of experiments on INS from molecular hydrogen. Of course, there are no rotations present in in the PdH_x system, and so any spectral contribution of the translational modes of H will be coupled with the vibrational modes of H against Pd.

In view ot the preceding experimental and theoretical considerations, a two-dimensional INS experiment to measure the $S(K, E)$ of PdH_x, e.g., in nanoparticles, would be worth studying. Depending on the neutron initial energy E_0 (say, a few 100 meV), various coupled vibrational-translational modes of atomic H become experimentally accessible. We again may expect a qualitatively similar anomaly as in the INS experiments on H_2 in C-nanotubes [24] (see Section 5), namely:

- INS measurements should reveal an anomalous momentum-transfer deficit on the H-atoms, being qualitatively similar to the effect of H_2 in nanoporous materials of Figure 5 discussed above. The vibro-translational quasi-continuum—being analogous to the roto-translational one [24]—should be again in the quantum domain of the $K - E$, i.e., "on the left" of the theoretical free-H recoil parabola.

Also in this case, the possible observation of any momentum transfer "anomalies" would shed new light onto the quantum interactions and dynamics of H with the host

metals, and reveal new aspects of their quantum nature that present-day quantum-chemical calculations cannot capture.

7.3. INS from Single H_2 in C_{60}

It is widely believed that INS is not subject to any selection rules; see e.g., the INS textbook [17]. However, an unexpected selection rule was recently discovered, which concerns the INS spectroscopy of a H_2 in a near-spherical confinement, i.e., a C_{60} fullerene. This new selection rule concerns the rotation-translation dynamics of the H_2 molecule in C_{60}, and results in certain forbidden INS roto-translational transitions of H_2 which have been also experimentally confirmed; see Refs. [32,33] and papers cited therein.

This INS topic is also of particular interest, if one recalls that the above investigated momentum-transfer deficit effect of H_2 in C-nanotubes (see Section 4) does also affect the roto-translational H_2-motion. Thus it seems natural to wonder, whether some anomalous momentum transfer might be present in the H_2-in-C_{60} system, too. Hence, in the light of the WV-TSVF theoretical model mentioned above,

- we may expect a related "anomalous" momentum transfer deficit in H_2-in-C_{60} too. Since the confinement provided by C_{60} allows only for a very small quasi-translation within the C_{60}-cage, we may expect that the expected quantum momentum-transfer deficit of measurable roto-translational peaks should be much less pronounced that in the case of H_2-in-C-nanotube (Section 4).

It may be noted that the quantum calculations reported in Ref. [32] can only calculate E-transfers, as all quantum chemical calculations do. But momentum transfers are beyond the reach of present-day numerical quantum chemical methods. This effect, if observable, will indicate a new aspect of the selection rule of rotation-translation INS-dynamics.

7.4. Momentum Transfer Deficit in Scattering by Multi-Layered Structures

Recently in Ref. [12] we suggested that the momentum-transfer deficit effect could probably be observed

(1) by *neutron reflectivity* from thin layers and/or coated surfaces of solid-liquid interfaces (e.g., Si/SiO_2/water), and
(2) *X-ray diffraction from crystalline structures* (e.g., Si and LaB_6 powders). Additionally, some preliminary measurements indicating a non-conventional component in the measured signals did provide some hints of the predicted new momentum-transfer deficit effect under consideration. In both these mentioned experimental fields, the expected deviations from conventional theory would have no conventional theoretical interpretation.

For some related preliminary data and results, the interested read may consult Ref. [12].

8. Additional Remarks and Discussion

The theory of WV and the TSVF are nowadays active areas of research, providing new conceptual ideas and suggesting new experiments within a wide range of fields. In the present paper, however, interpretational issues are briefly mentioned only; see e.g., Appendix B. Instead, the focus is a new family of experiments related to momentum and/or energy transfers, thus contributing to the connection between the "theory"-community and that of experimental neutron scattering.

This novel theoretical frame reveals several counter-intuitive effects which may appear "strange" or even "wrong", since, e.g.,—in view of the conventional neutron scattering theory [9]—they seem to violate the basic conservation laws of energy and momentum. In order to remove this and similar misunderstandings, and to facilitate further understanding, here we make several additional remarks and/or provide related explanations.

(A) We have discussed in detail why the striking experimental INS observations of Section 5 appear to be "anomalous" (i.e., they have no interpretation) in the frame of

standard INS theory. In this context, one may believe that these observations can also be interpreted within "standard" formalism of QM, i.e without the need to apply WV and TSVF (as proposed in Section 6). In other terms, it is conceivable that standard INS theory could be *properly extended*, with the aim to interpret the INS observations using only "traditional" quantum theoretical terms.

Of course, our present work does not exclude this possibility. However, in the light of the detailed discussions of Section 4, it should be clear that any such extension of conventional INS theory has to violate and/or replace (some of) the basic INS-theoretical conditions $A1$–$A5$. Such an extension is unknown thus far.

(B) In some theoretical papers one finds the criticism that post-selection just means "throwing out some data", and thus that weak values are not inherently quantum but rather a purely statistical feature of pre- and post-selection with disturbance; cf. [34]. As an example of other criticisms, see e.g., the early comment [35] on the original paper [2]. Furthermore, it has been argued that the conditions under which WV can be related to the system properties are rather stringent; for a recent discussion, the interested reader is referred to Ref. [36].

In the experimental context of INS and related scattering experiments discussed above, however, post-selection certainly corresponds to "performing a concrete measurement on a well positioned sample (with respect to the neutron beam direction), using a well defined detector, and analyzing the thus measured data only"; see e.g., the experiments in Section 5. The many applications and/or new predicted effects of WV-TSVF clearly support the viewpoint that post-selection is a genuine physical concept. Furthermore, and more specifically, the short analysis of the photon-mirror collision in a MZI, as presented in Section 2.1, provides considerable evidence that the TSVF part of the theory is an indispensable tool for the understanding of some new phenomena.

Recently, de Castro et al. [37] provided a broader theoretical frame of weak values and advanced formal collision theory [38], aiming to apply it in various experimental set-ups as e.g., in the case of ultracold atomic collisions.

(C) Nowadays it is recognized that a Weak Value is a unique quantum interference phenomenon of a single system with itself; see e.g., [39]. As the above INS experiments and their interpretation strongly indicate, a WV is a novel robust and well-defined property of a single pre- and post-selected quantum system. WVs may also play a direct role in the quantum dynamics of a single system. Consequently, a WV value appears to have a physical meaning beyond a conditional average of a pointer in a weak measurement procedure [40].

(D) The fact that the neutron-H collision is not immediately recognized to correspond to a weak measurement (WM)—which is believed to be a prerequisite for the applicability of WV-theory—was discussed in some detail in the original paper [11]. Here it suffices to note the following points. Generalizing the WM formalism, Oreshkov and Brun [41] showed that WMs are universal, in the sense that any generalized measurement can be decomposed into a sequence of appropriately designed weak measurements. This interesting theoretical result may have important applications to various topics, like e.g., the INS process under consideration. In this context, a remarkable finding of Cohen and Pollak [42] should be mentioned, which says that, in principle, a WV can also be determined by strong (projective) measurements of suitably defined Hermitian operators.

Additionally, the experimental and theoretical investigations by Dziewior et al. [43] may be mentioned, which also explicitly apply the formalism of WVs to the case of much stronger interactions than WMs. Here the authors obtain a novel expression for WVs which takes into account changes due to interactions of finite strength in the time interval between pre- and post-selection. Moreover, besides incorporating the stronger interactions, the formalism also accounts for decoherence and/or imperfections in the measurement system [43].

Summarizing, weak values are general properties of observables (operators) in association with the physical concepts of pre- and post-selection, and there is no need to associate them with WMs only.

(E) These views are also in line with the following specific observation. In our theoretical model of Section 6, the two operators $\hat{q}$ and $\hat{P}$ occurring in the von Neumann-type interaction Hamiltonian of Equation (20) refer to two *different* quantum systems. Thus, as Vaidman [44] pointed out, the concept of WV arises here due to the interference of a quantum entangled wave and therefore it has no analog in classical wave interference. This further supports the conclusion that WV is a genuinely quantum concept and not some kind of "approximation".

(F) In contrast to our WV-TSVF model, conventional neutron scattering theory [9,16,17] treats the neutron as a classical plane wave, i.e., no dynamical variables of the neutron appear in the derivations and the main theoretical results. e.g., consider the basic formula for the partial differential cross-section, which includes the dynamic structure factor $S(K, E)$ of the scattering system. This contains degrees-of-freedom of the scatterer only—the neutron is "downgraded" to a classical object and only the scattering length b_A (a *c*-number) describing the neutron-atom interaction appears here.

Moreover, let us also mention shortly that, in the conventional theory and experimental practice of neutron scattering, the *coherence length* of the neutron is believed to be fully irrelevant; cf. e.g., the above cited references. However, as one could conjecture in the light of the anomalous momentum-transfer deficit effect, this belief becomes questionable.

(G) The momentum transfer deficit, and the associated "anomalous" effective-mass reduction of the scattering particle, say H, might be seen to violate the energy and momentum conservation laws of basic physics. However, as already stressed above, this is not the case, because the neutron-H system is not a closed, but an *open* quantum system. Thus we may say that the participation of H's environment to the neutron-H scattering dynamics is indispensable for the new WV-TSVF effect under consideration. In other terms, the correct conservation relations should read

$$E_{H+\mathcal{E}} = -E_n \quad \text{and} \quad \hbar\mathbf{K}_{H+\mathcal{E}} = -\hbar\mathbf{K}_n, \tag{33}$$

which are valid in the case that the environment $\mathcal{E}$ of the scattering H is present; see also Appendix A. In contrast, the common view (at least for experimenters) in this context is quite different: One believes that it holds $E_H = -E_n$ and $\mathbf{K}_H = -\hbar\mathbf{K}_n$, mainly based on the belief that the n-proton scattering is extremely fast, or even "instantaneous"; see also Appendix A.

(H) Moreover, let us mention in this context the very recent publication by Aharonov et al. [45] regarding a revealing theoretical analysis of the very meaning of the basic conservation laws of quantum mechanics. The reason for doing this, in connection with the momentum-transfer deficit effect of the present paper, is the following stimulating physical insight:

> "Energy ... is a property of an entire wave function. However, the law of conservation of energy is often applied to processes in which a system with an extended wave function interacts with a local probe. How can the local probe "see" an extended wave function? What determines the change in energy of the local probe? These questions lead us to uncover quantum processes that seem, paradoxically, not to conserve energy" [45], p. 1.

Here one may easily recognize an (intuitive, at least) analogy with the specifics of our INS process. Namely, in the case of H_2 in C-nanotubes, a neutron interacts with a proton "locally" (since the Fermi-pseudo-potential has a range of some 10^{-15} m [9]), whereas the wavefunction of the roto-translating H_2 is extended over a few Å, which is ca. 10^5 times larger.

(I) Quantum interference and entanglement [46] have been recognized to be crucial for quantum computing and quantum information theory; cf. [47] and the very recent

Refs. [48,49]. Hence it would be interesting to explore a potential applicability of the new quantum features offered by WV-TSVF to recently emerging fields of quantum computational complexity theory [50] and ICT (information and communication technology). Namely, WV-TSVF appears to make possible the exploration of *a new kind of quantum information*—like e.g., the correlation between momentum transferred on the mirror *M* and the photon measured with detector D_2 in the example of Section 2.

(J) In view of the experimentally detected effective-mass reduction, Section 5, it seems appropriate to mention here some speculative ideas concerning a possible technological importance of the new theory. Namely, H^+ mobility concerns the properties of fuel cells (hydrogen technology) and carbon-based materials for H-storage. Cf. the proposed experiment in Section 7.1.

(K) In view of the above discussions and experimental INS results, one may arrive at the following point of considerable interest: The quantum nature of nuclei (here: protons) may be far more important, and more widely present, that realized thus far. The strong roto-translational "anomaly" of H_2 in C-nanotubes indicates that the H-substrate interactions are far more complex than the common quantum-chemical calculations can capture. (The latter consider only the electrons as quantum objects.) In other terms, it seems that the importance of the quantum nature of protons for the chemical properties of H/surface interactions (and thus also on the chemical bonding in general) should be reconsidered.

Concluding, we believe that the theoretical formalism of WV and TSVF not only sheds new light on interpretational issues of fundamental quantum concepts (like e.g., the time-inversion invariance of the basic physical laws, the meaning of quantum entanglement and correlations, etc.) but it also offers a fascinating new guide for our intuition to predict new effects, and further helps to design and perform new experiments and reveal novel quantum phenomena.

Funding: This research received no external funding.

Data Availability Statement: No new data were created or analyzed in this study.

Acknowledgments: I wish to thank Bill Poirier (Texas Tech Univ.) for stimulating discussions and bringing into my attention the research topic "$H_2@C_{60}$ and an inelastic neutron scattering selection rule", and the unknown reviewers for constructive criticisms and insightful remarks.

Conflicts of Interest: The author declares no conflict of interest.

Abbreviations

The following abbreviations are used in this manuscript:

a.m.u.	atomic mass unit
DFT	Density Functional Theory
IA	Impulse Approximation
INS	Incoherent Inelastic Neutron Scattering, also denoted by IINS
ICT	Information and Communication Technology
MZI	Mach-Zehnder Interferometer
QM	Quantum Mechanics
WV	Weak Value
WM	Weak Measurement
TSVF	Two-State Vector Formalism
TOF	Time-of-Flight
DINS	Deep-Inelastic Neutron Scattering
NCS	Neutron Compton Scattering, equivalent to DINS
XRD	X-ray Diffraction

Appendix A. Scattering Spectrometer and "What Is Directly Measured"

Appendix A.1. Introductory Remarks

Certain instrumental details are crucial for understanding the obtained results and assessing their meaning. In this section we deal with the question of "what is directly measured" in the experiment (i.e., independently from individual theoretical assumptions and/or one's beliefs), and what is derived from the measured data.

First of all, let us note the following fact. A typical neutron scattering experimental setup should measure the dynamical structure factor $S(K, E)$ of the scatterer; see e.g., [9]. So, the values of K and E refer to the scattering particles, say H atoms (protons), as in the INS experiments of this paper. However, these are not directly measured because, as a matter of fact, directly measured are these quantities *of the neutron*; see below. So, one must "derive" from the measured data the needed K and E values of H entering the function $S(K, E)$.

We consider *isotropic* scattering only, so that only one angle (i.e., θ) appears in the scattering expressions.

The kinetic energies (say, less than 1 eV) of the neutrons in these experiments imply that all effects under consideration, as well as their theoretical analysis, belong to *non-relativistic* theory.

A self-contained and more detailed presentation of the TOF experimental procedure may be found in Refs. [11–13].

Appendix A.2. TOF-Spectrometers and Incoherent Inelastic Neutron Scattering from H Atoms

The newest generation neutron scattering spectrometers are Time-of-Flight (TOF) instruments; cf. Figure A1. Here, a short pulse of neutrons reaches the first monitor of the spectrometer, which triggers the measurement of TOF. Subsequently, a neutron scatters from the sample and may reach the detector, which stops the TOF measurement. Modern neutron TOF-spectrometers, like e.g., ARCS [19], have several thousand individual detectors (called detector pixels).

Here, as also in the whole paper, we consider isotropic scattering only.

From each TOF-value measured with an individual detector at scattering angle θ, the associated transfers of momentum ($\hbar K$) and energy ($E = \hbar\omega$) caused by the collision of the neutron with the scatterer are uniquely determined; see, e.g., [11]. Below we will see that each TOF-value corresponds uniquely to one pair of K and E values. Moreover, each detector measures around one specific trajectory in the whole plane of momentum and energy transfers $K - E$. (This abbreviation is commonly used, instead of the more precise $\hbar K - E$.)

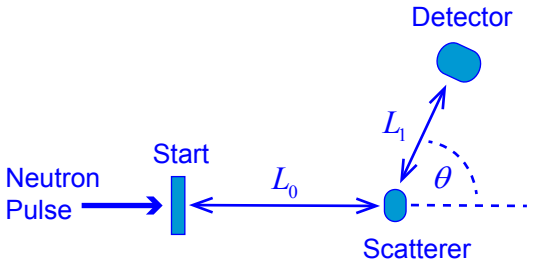

Figure A1. Scheme of a time-of-flight neutron scattering setup. (Taken from [11], with permission of *Quanta*).

Appendix A.3. Details of Scattering Spectrometer, Calibration and "What Is Measured"

A schematic setup of a standard TOF scattering experiment is as follows; cf. Figure A1. A short pulse of neutrons produced by the neutron spallation source (e.g., SNS, USA) reaches the monitor, that is, the clock that starts the TOF measurement). L_0 is the distance between monitor and sample. A scattered neutron of the pulse reaches the detector which

triggers the stop signal of the TOF measurement. L_1^θ (or L_1, for simplicity) is the sample–detector distance; the corresponding scattering angle is θ. Here we consider isotropic scattering only.

A measured TOF value t_{TOF} is given by

$$t_{TOF} = \frac{L_0}{v_0} + \frac{L_1^\theta}{v_1} + t_0 \tag{A1}$$

(v_0 and v_1: velocities of the neutron before and after scattering, respectively; t_0: a time-offset parameter due to the electronics.)

In most cases, v_0 and thus also E_0 have predetermined fixed values, and then one speaks of a "direct geometry" TOF-spectrometer. ARCS and MARI, used for some of the aforementioned experiments, are such spectrometers.

We consider now the kinematics of incoherent neutron scattering. The scattering intensity measured by a detector is a function of the neutron's energy transfer

$$\begin{aligned} E = E_0 - E_1 \equiv \hbar\omega &= \frac{1}{2}mv_0^2 - \frac{1}{2}mv_1^2 \\ &= \frac{(\hbar k_0)^2}{2m} - \frac{(\hbar k_1)^2}{2m} \end{aligned} \tag{A2}$$

(m: neutron mass) and the corresponding momentum transfer on the neutron caused by the collision

$$\hbar\mathbf{K}_n = \hbar\mathbf{k}_1 - \hbar\mathbf{k}_0 \tag{A3}$$

(As usual, here bold letters represent vectors, and italics denote scalars.) One has

$$|\mathbf{K}_n| = K_n = \sqrt{k_0^2 + k_1^2 - 2k_0k_1\cos\theta} \tag{A4}$$

where k_i is the modulus of vector $\mathbf{k}_i$.

Since we consider here *incoherent* [9,10] scattering, the exchange of momentum and energy is between a neutron and (better: the nucleus of) a single atom [9,10]. The neutron-H scattering is overwhelmingly incoherent [9]. Due to Newton's "actio = reactio", in strict two-body scattering the struck atom (nucleus) receives the momentum transfer

$$\mathbf{K}_A = -\mathbf{K}_n \tag{A5}$$

and it holds:

$$K \equiv |\mathbf{K}_A| = |\mathbf{K}_n| \tag{A6}$$

Since the sample is initially at rest, each neutron scatters from an atom with mass M and zero mean initial momentum, i.e., $\langle P \rangle = 0$. Due to the conservation of kinetic energy and momentum *in a binary collision*, it holds the kinematic relation (the same as in classical mechanics)

$$\frac{k_1}{k_0} = \frac{\cos\theta + \sqrt{(M/m)^2 - \sin^2\theta}}{M/m + 1} \tag{A7}$$

which is the same as in classical mechanics.

The following facts should be emphasized.

(a) The measured energy and momentum transfer values are those *of the neutron*—and not those of the struck atom, in our case H.

(b) From the measured TOF value (A1) follow the values of v_1, Equation (A1), of $k_1 = |\mathbf{k}_1|$, and consequently of energy transfer $E = \hbar\omega$, see Equation (A2). Note that the value of θ plays no role in the determination of E-transfer. In other words, the E-value —for each single elementary scattering process—is independent of any tacit theoretical beliefs or assumptions, because it follows from the actually measured TOF value directly.

(c) Momentum transfer $\hbar\mathbf{K}$, Equation (A4), is determined from both the measured TOF value and the direction θ in which the detector is placed. Regretfully, the direct experimental determination of θ (which is given by the geometry of the spectrometer) is by no means a simple matter. Furthermore, one uses Equation (A7) which connects the value of θ and the atomic mass M. In other words, one takes for granted that the atomic mass of M is well known—recall that non-relativistic quantum mechanics holds here—and thus the conventionally expected ratio k_1/k_0 is fully determined.

The following point is crucial: Since the scattering H atoms in our experiments are not free particles in empty space, but interacting with their local environment, the quantity M appearing in the above kinematic equations may be expected to be different from that of the free H atoms. This point is crucial to note, since it is quite often a common practice to use the free-mass M-value in order to "fine-tune" and/or "improve" the calibration of the instrument, i.e., to "optimize" the instrumental values of θ and L_1 (for all detectors). The aim of this is to achieve an agreement of the measured scattering data with conventional scattering theory; for a detailed example see [51]. In particular, this is often done for scattering data from H, since the H-neutron scattering θ-dependence is very sensitive to θ, as Equation (A7) shows. For a detailed discussion and experimental examples, cf. [51,52].

The common justification for doing this "improvement of calibration" is roughly as follows: The impulsive neutron-nucleus interaction is ultra-short, due to the very small range of the Fermi pseudo-potential of the strong force (ca. in the femto-meter range), and the limited velocity (say, 1–10 km/s) of a thermal neutron. Thus the struck atom has no time to change its position during the collisional time and "feel" the environmental forces, and thus it behaves as being "free" during the collision. This view is based on the belief that the and strictly impulsive two-body neutron-nucleus collision is a valid assumption, and thus the free-atom mass is the correct quantity for the parameter M entering the kinematic Equations (A1)–(A7).

Let us summarize the above considerations as follows. From each measured t_{TOF} in direction θ, the corresponding momentum ($\hbar K$) and energy ($E = \hbar\omega$) transfers (between neutron and scatterer) are uniquely determined. Thus one also sees that each specific detector measures one specific trajectory, or a narrow band around it, in the two-dimensional $K - E$ plane.

According to Equations (A2) and (A4), the detector's instrumental parameters $\{\mathrm{IP}\}$ shown in Equation (A1) determine the corresponding scattering intensity $I(\mathbf{K}, E)$ and the corresponding dynamical structure factor $S(\mathbf{K}, E)$ of the scattering system. The latter is the key quantity for the theoretical analysis of experimental data [9]. In short:

$$I(\mathrm{TOF}, \{\mathrm{IP}\}) \;\Rightarrow\; I(\mathbf{K}, E) \;\Rightarrow\; S(\mathbf{K}, E) \tag{A8}$$

However, as they stand, these relations are ambiguous and/or misleading, because the measured quantities $\mathbf{K}$ and E are those of the neutron, and *not of the scattering particle*, i.e., H, in our INS case. I.e., one needs to determine $\mathbf{K}_H$ and E_H referring to the struck H (and not to the whole scattering sample).

But $\mathbf{K}_H$ and E_H are not directly measurable, since the struck H is a part of a condensed (or complex) system. Hence, one may obtain the desired dynamical structure factor $S(\mathbf{K}_H, E_H)$ only with some additional theoretical assumption, like e.g., the conventionally done approximations

$$E_H = -E_n \quad \text{and} \quad \hbar\mathbf{K}_H = -\hbar\mathbf{K}_n, \tag{A9}$$

which express energy and momentum conservation only for an idealized *closed* two-body neutron-H system. But these are incorrect in our INS context, because they ignore the existence and the dynamical role of the environment $\mathcal{E}$ of H, which is the reason for the "anomalous" character of the scattering effect under consideration.

In other words, H, and also the two-body system "neutron + H" are open quantum systems. Thus one may write down explicitly the conservation relations for the complete closed system "neutron + H + $\mathcal{E}$"

$$E_{H+\mathcal{E}} = -E_n \quad \text{and} \quad \hbar\mathbf{K}_{H+\mathcal{E}} = -\hbar\mathbf{K}_n, \tag{A10}$$

which express the correct energy and momentum conservations for a closed system. Clearly, if one neglects $\mathcal{E}$ (or over-simplifies its quantum character), the conservation laws seem artificially violated. Hence we can say that the quantum dynamics of $\mathcal{E}$ is indispensable for the interpretation of the considered "anomalous" INS effect from H.

Appendix B. On the Elitzur-Vaidman Effect, Quantum Processor, and Implications for the Logical-Axiomatic Status of the Wavefunction

As already mentioned above, it should be emphasized that "interpretational issues" of quantum mechanics, and especially of the quantum term "wavefunction" (or state vector; we do not differentiate between the two here) are not in the focus of this paper. Nevertheless, the experimental findings and their theoretical interpretation presented below, appear to shed more light on such issues, and, moreover, may provide further physical insight into, and contribute to the understanding of, the WV-TSVF theoretical framework.

As rather broadly believed even today, a wavefunction is considered to describe an *ensemble* of (identical) quantum systems, e.g., molecules, rather than a single quantum system. This implies that the wavefunction should be understood as a purely epistemological term, i.e., as a mathematical term representing the observer's knowledge about the quantum ensemble. In contrast, and due to the tremendous progress of physical instrumentation which permits to make experiments with single quantum systems (e.g., single atoms), the recently emerging viewpoint is to consider the wavefunction as an ontological entity of *single* systems, that is, as a real and objective physical entity—rather in the same sense as the values of momentum or energy of a single system. The latter is also the viewpoint supported by the novel WV-TSVF theory.

On the Elitzur-Vaidman effect—This counter-intuitive quantum effect [53] (sometimes known as "bomb-tester"), and the associated *interaction-free* measurements (IFM), give strong support to the real nature of wavefunction. This fundamental thought experiment revealed the ability to gain information about an object's (or "bomb's") presence in one of the two paths within a Mach-Zehnder interferometer (MZI) without ever "touching" it. Within classical physics this is impossible, for the following plain reason. In the case a successful interaction-free "bomb detection", no known physical quantity—e.g., energy, momentum, angular momentum, force, etc.—has been exchanged between the probe particle (or photon) entering the MZI and the "bomb"). This physical information, which is a classical record, however, cannot be reached "at no costs" at all. The only possible conclusion is that the necessary "costs" are provided by the wavefunction of the probe. This predicted novel quantum effect (in the meantime also experimentally confirmed) strongly demonstrates that the wavefunction is a real physical entity—and not just an auxiliary quantity being used in order to perform calculations (e.g., of mean values of real physical quantities like e.g., energies or momenta).

On GOOGLE*'s quantum processor*—Very recently, the interpretation of the quantum wavefunction as a real physical entity became relevant for experimental and industrial applications, e.g., quantum cryptography and quantum computation. In this context one may refer to the technological achievement to demonstrate experimentally the so-called "quantum supremacy", using GOOGLE's programmable quantum processor *Sycamore* with 53 qubits, which executes a specific computational task [48]. The authors of this paper report a (very specific) quantum computational task being executed in about 200 seconds—in contrast to the estimated 10,000 years needed by the (presently existing) most powerful classical supercomputer in order to perform the same task. Here, the wavefunctions calculated by the quantum processor play a central role. To put it in plain terms, we may say that any wavefunction calculated by the GOOGLE processor is a physical quantity of a

single quantum processor (i.e., a single quantum system)—and certainly *not* of an ensemble of quantum processors.

As an additional related example, we may mention a recent achievement using quantum optical technology [49], in which boson sampling—using 20 photons in a 10^{14}-dimensional Hilbert space—was applied towards demonstrating the the aforementioned "quantum supremacy" of quantum computing over classical computing. Again, also here each one calculated wavefuction represents a single quantum optical setup—and not an ensemble of such setups.

On Si quantum photonic chip technology—A remarkable technological advance was recently provided by the integration of three resonance-enhanced photon-pair sources, interferometers, and other quantum gates and components, on a single monolithic silicon chip [54]. The experiments demonstrated high-visibility quantum interference and the production of high-quality path-entangled-qutrit states. Various questions concerning nonlocality, contextuality and other fundamental properties of quantum theory have been successfully addressed. Moreover, a fundamental problem of computational theory (i.e., the Perfect Matching of theory of graphs) has been experimentally approached. Although the structure of the graph under study was very simple, this work can be viewed as a first step towards achieving the ambitious goal of solving a #P hard problem [50] applying quantum photonic devices.

Obviously, the many-particle wavefunction operating in these experiments refers to a single quantum system, i.e., the monolithic Si chip created by the authors.

On Density Functional theory—A part of the scientists working with numerical quantum chemical methods seem to believe that the wavefunction is not a fundamental entity, because, in cases the well known density functional theory (DFT) can be applied, the wavefunction can be replaced with a so-called density functional. This simplified method makes possible to calculate various properties of molecular systems with a huge number of atoms—something that the numerical treatment of the Schrödinger equation with present-day computers cannot achieve. However, this belief is is not quite correct. Namely, Norden writes in an Editorial entitled "Which are the 'Hilbert Problems' of Biophysics?" [55], the following remarks: "According to a theorem by Kohn and Hohenberg, an electron density functional always exists that can electrostatically uniquely define a molecular ground state without need for consideration of Schrödinger wavefunctions. However, despite this existence proof, nobody has yet been able to produce such a density functional, and so-called DFT methods do not rest on true Density Functionals." [55], p. 3.

Additionally, it may be noted that DFT addresses structural (i.e., static) problems, and not problems of quantum dynamics. In quantum dynamics, the quantum phase of the wavefunction is of paramount importance, but it plays a minor role in electrostatics. Needless to say that the operations of a quantum processor cannot be described using density functionals instead of wavefunctions.

Concluding, we believe that the above remarks strongly support the view that the concept of wavefunction represents a fundamental property of single quantum systems. See also the recent review article by Leifer [56].

References

1. Aharonov, Y.; Rohrlich, D. *Quantum Paradoxes: Quantum Theory for the Perplexed*; WILEY-VCH: Weinheim, Germany, 2005.
2. Aharonov, Y.; Albert, D.Z.; Vaidman, L. How the result of a measurement of a component of a spin 1/2 particle can turn out to be 100? *Phys. Rev. Lett.* **1988**, *60*, 1351–1354. [CrossRef] [PubMed]
3. Dressel, J.; Malik, M.; Miatto, F.M.; Jordan, A.N.; Boyd, R.W. Colloquium: Understanding quantum weak values: Basics and applications. *Rev. Mod. Phys.* **2014**, *86*, 307–316. [CrossRef]
4. Aharonov, Y.; Cohen, E.; Waegell, M.; Elitzur, A.C. The weak reality that makes quantum phenomena more natural: Novel insights and experiments. *Entropy* **2018**, *20*, 854. [CrossRef]
5. Tamir, B.; Cohen, E. Introduction to weak measurements and weak values. *Quanta* **2013**, *2*, 7–17. [CrossRef]
6. Shikano, Y. Theory of "Weak Value" and Quantum Mechanical Measurements. In *Measurements in Quantum Mechanics*; Pahlavani, M.R., Ed.; InTech: Shanghai, China; Rijeka, Croatia, 2012; pp. 75–100.

7. Aharonov, Y.; Cohen, E.; Elitzur, A.C. Foundations and applications of weak quantum measurements. *Phys. Rev. A* **2014**, *89*, 052105. [CrossRef]
8. Aharonov, Y.; Botero, A.; Nussinov, S.; Popescu, S.; Tollaksen, J.; Vaidman, L. The classical limit of quantum optics: Not what it seems at first sight. *New J. Phys.* **2013**, *15*, 093006. [CrossRef]
9. Squires, G.L. *Introduction to the Theory, of Thermal Neutron Scattering*, 2nd ed.; Cambridge Univ. Press: Cambridge, UK, 2012.
10. Feynman, R.P.; Leighton, R.B.; Sands, M. *The Feynman Lectures on Physics, Vol. III, Quantum Mechanics*; Addison-Wesley: Reading, MA, USA, 1965.
11. Chatzidimitriou-Dreismann, C.A. Weak measurement and Two-State-Vector formalism: Deficit of momentum transfer in scattering processes. *Quanta* **2016**, *5*, 61–84. [CrossRef]
12. Chatzidimitriou-Dreismann, C.A. Weak values and two-state-vector formalism in elementary scattering and reflectivity—A new effect. *Universe* **2019**, *5*, 58. [CrossRef]
13. Chatzidimitriou-Dreismann, C.A. Quantum Confinement Effects of Hydrogen in Nanocavities—Experimental INS Results and New Insights. *Recent Prog. Mater.* **2020**, *2*, 1–53. [CrossRef]
14. Chatzidimitriou-Dreismann, C.A. Experimental Implications of Negative Quantum Conditional Entropy—H_2 Mobility in Nanoporous Materials. *Appl. Sci.* **2020**, *10*, 8266. [CrossRef]
15. Ashcroft, N.W.; Mermin, N.D. *Solid State Physics*; Saunders College RHW: Philadelphia, PA, USA, 1976.
16. Watson, G.I. Neutron Compton scattering. *J. Phys. Condens. Matter* **1996**, *8*, 5955–5975. [CrossRef]
17. Mitchell, P.C.H.; Parker, S.F.; Ramirez-Cuesta, A.J.; Tomkinson, J. *Vibrational Spectroscopy with Neutrons*; World Scientific: Singapore, 2005.
18. Diallo, S.O.; Azuah, R.T.; Abernathy, D.L.; Rota, R.; Boronat, J.; Glyde, H.R. Bose–Einstein condensation in liquid ^{4}He near the liquid-solid transition line. *Phys. Rev. B* **2012**, *85*, 140505. [CrossRef]
19. Available online: https://neutrons.ornl.gov/ARCS (accessed on 26 February 2021).
20. Kofu, M.; Yamamuro, O. Dynamics of atomic hydrogen in palladium probed by neutron spectroscopy. *J. Phys. Soc. Jpn.* **2020**, *89*, 051002. [CrossRef]
21. Chatzidimitriou-Dreismann, C.A. Quantumness of correlations and Maxwell's demon in molecular excitations created by neutron scattering. *Int. J Quantum Chem.* **2015**, *115*, 909–929. [CrossRef]
22. Available online: https://www.isis.stfc.ac.uk/Pages/mari.aspx (accessed on 26 February 2021).
23. Kearley, G.J.; Fillaux, F.; Baron, M.H.; Bennington, S.; Tomkinson, J. A new look at proton transfer dynamics along the hydrogen bonds in amides and peptides. *Science* **1994**, *264*, 1285–1289. [CrossRef]
24. Olsen, R.J.; Beckner, M.; Stone, M.B.; Pfeifer, P.; Wexler, C.; Taub, H. Quantum excitation spectrum of hydrogen adsorbed in nanoporous carbons observed by inelastic neutron scattering. *Carbon* **2013**, *58*, 46–58. [CrossRef]
25. Callear, S.K.; Ramirez-Cuesta, A.J.; David, W.I.F.; Millange F.; Walton, R.I. High-resolution inelastic neutron scattering and neutron powder diffraction study of the adsorption of dihydrogen by the Cu(II) metal–organic framework material HKUST-1. *Chem. Phys.* **2013**, *427*, 9–17. [CrossRef]
26. Aharonov, Y.; Cohen, E.; Ben-Moshe, S. Unusual interactions of pre-and-post-selected particles. *EPJ Web Conf.* **2014**, *70*, 00053. [CrossRef]
27. Turrillas, X.; Delabouglise, G.; Joubert, J.G.; Fournier, T.; Muller, J. Un nouveau conducteur protonique $H_3OSbTeO_6$, xH_2O. Conductivite en fonction de la temperature et de la pression partielle de vapeur d'eau. *Solid State Ionics* **1985**, *17*, 169–174. [CrossRef]
28. Boysen, H.; Lerch, M.; Fernandez-Alonso, F.; Krzystyniak, M.; Lalowicz, Z.T.; Chatzidimitriou-Dreismann, C.A.; Tovar, M. On the mechanism of proton conductivity in $H_3OSbTeO_6$. *J. Phys. Chem. Solids* **2012**, *73*, 808–817. [CrossRef]
29. Anovitz, L.M.; Mamontov, E.; Ben Ishai, P.; Kolesnikov, A.I. Anisotropic dynamics of water ultraconfined in macroscopically oriented channels of single-crystal beryl: A multifrequency analysis. *Phys. Rev. E* **2013**, *88*, 052306. [CrossRef]
30. Krzystyniak, M.; Abdul-Redah, T.; Lerch, M.; Chatzidimitriou-Dreismann, C.A. *Neutron Compton Scattering on $H_3OSbTeO_6$*; ISIS Experimental Report; Unpublished Work, 2012.
31. Fukai, Y. *The Metal-Hydrogen System*, 2nd ed.; Springer: Berlin/Heidelberg, Germany; New York, NY, USA, 2005; pp. 1–512.
32. Xu, M.; Ye, S.; Powers, A.; Lawler, R.; Turro, N.J.; Bačić, Z. Inelastic neutron scattering spectrum of H_2@C60 and its temperature dependence decoded using rigorous quantum calculations and a new selection rule. *J. Chem. Phys.* **2013**, *139*, 064309. [CrossRef] [PubMed]
33. Poirier, B. Communication: The $H_2@C_{60}$ inelastic neutron scattering selection rule: Expanded and explained. *J. Chem. Phys.* **2015**, *143*, 101104. [CrossRef]
34. Ferrie, C.; Combes, J. How the result of a single coin toss can turn out to be 100 heads. *Phys. Rev. Lett.* **2014** , *113*, 120404. [CrossRef] [PubMed]
35. Leggett, A.J. Comment on "How the Result of a Measurement of a Component of the Spin of a Spin-1/2 Particle Can Turn Out to be 100". *Phys. Rev. Lett.* **1989**, *62*, 2325. [CrossRef]
36. Matzkin, A. Weak values and quantum properties. *Found. Phys.* **2019**, *49*, 298–316. [CrossRef]
37. de Castro, L.A.; Brasil C.A.; de Jesus Napolitano, R. Weak values in collision theory. *Ann. Phys.* **2018**, *392*, 272–286. [CrossRef]
38. Taylor, J.R. *Scattering Theory: The Quantum Theory of Nonrelativistic Collisions*; Wiley: New York, NY, USA, 1972.
39. Dressel, J. Weak values as interference phenomena. *Phys. Rev. A* **2015**, *91*, 032116. [CrossRef]

40. Vaidman, L.; Ben-Israel, A.; Dziewior, J.; Knips, L.; Weissl, M.; Meinecke, J.; Schwemmer, C.; Ber, R.; Weinfurter, H. Weak value beyond conditional expectation value of the pointer readings. *Phys. Rev. A* **2017**, *96*, 032114. [CrossRef]
41. Oreshkov, O.; Brun, T.A. Weak measurements are universal. *Phys. Rev. Lett.* **2005**, *95*, 110409. [CrossRef]
42. Cohen, E.; Pollak, E. Determination of weak values of quantum operators using only strong measurements. *Phys. Rev. A* **2018**, *98*, 042112. [CrossRef]
43. Dziewior, J.; Knips, L.; Farfurnik, D.; Senkalla, K.; Benshalom, N.; Efroni, J.; Meinecke, J.; Bar-Ad, S.; Weinfurter, H.; Vaidman, L. Universality of local weak interactions and its application for interferometric alignment. *Proc. Natl. Acad. Sci. USA* **2019**, *116*, 2881–2890. [CrossRef] [PubMed]
44. Vaidman, L. Comment on "How the result of a single coin toss can turn out to be 100 heads". *arXiv* **2014**, arXiv:1409.5386.
45. Aharonov, Y.; Popescu, S.; Rohrlich, D. On conservation laws in quantum mechanics. *Proc. Natl. Acad. Sci. USA* **2021**, *118*, e1921529118. [CrossRef] [PubMed]
46. Horodecki, R.; Horodecki, P.; Horodecki, M.; Horodecki, K. Quantum entanglement. *Rev. Mod. Phys.* **2009**, *81*, 865–942. [CrossRef]
47. Nielsen, M.A.; Chuang, I.L. *Quantum Computation and Quantum Information*; Cambridge University Press: Cambridge, UK, 2010.
48. Arute, F.; Arya, K.; Babbush, R.; Bacon, D.; Bardin, J.C.; Barends, R.; Biswas, R.; Boixo, S.; Brandao, F.G.; Buell, D.A.; et al. Quantum supremacy using a programmable superconducting processor. *Nature* **2019**, *574*, 505–510. [CrossRef] [PubMed]
49. Wang, H.; Qin, J.; Ding, X.; Chen, M.C.; Chen, S.; You, X.; He, Y.M.; Jiang, X.; You, L.; Wang, Z.; et al. Boson sampling with 20 input photons and a 60-mode interferometer in a 10^{14}-dimensional Hilbert space. *Phys. Rev. Lett.* **2019**, *123*, 250503. [CrossRef] [PubMed]
50. Arora, S.; Barak, B. *Computational Complexity—A Modern Approach*; Cambridge University Press: Cambridge, UK, 2009.
51. Chatzidimitriou-Dreismann, C.A.; Gray, E.; Mac, A.; Blach, T.P. Distinguishing new science from calibration effects in the electron-volt neutron spectrometer Vesuvio at ISIS. *Nucl. Instrm. Meth. A* **2012**, *676*, 120–125. [CrossRef]
52. Chatzidimitriou-Dreismann, C.A.; Gray, E.M.; Blach, T.P. Indications of energetic consequences of decoherence at short times for scattering from open quantum systems. *AIP Adv.* **2011**, *1*, 022118. [CrossRef]
53. Elitzur, A.C.; Vaidman, L. Quantum mechanical interaction-free measurements. *Found. Phys.* **1993**, *23*, 987–997. [CrossRef]
54. Lu, L.; Xia, L.; Chen, Z.; Chen, L.; Yu, T.; Tao, T.; Ma, W.; Pan, Y.; Cai, X.; Lu, Y.; et al. Three-dimensional entanglement on a silicon chip. *npj Quantum Inf.* **2020** *6*, 30. [CrossRef]
55. Norden, B. Which are the 'Hilbert Problems' of biophysics? *QRB Discov.* **2021**, *2*, 1–3. [CrossRef]
56. Leifer, M.S. Is the quantum state real? An extended review of ψ-ontology theorems. *Quanta* **2014**, *3*, 67–155. [CrossRef]